CAUSALITY IN TURBULENCE AND TRANSITION

Universidad Politécnica Madrid, May 3-5, 2022

Programme and Book of Abstracts

Scientific committee

Oscar Flores
Dan Henningson
Gianluca Iaccarino
Javier Jiménez
Detlef Lohse
Adrián Lozano-Durán
Genta Kawahara
Rich Kerswell
Peter J. Schmid

Invited speakers

Genta Kawahara
Petros Koumoutsakos
Mark J. Rodwell
Jakob Runge
Kunihiko Taira

Local committee

Javier Jiménez
Miguel P. Encinar
Kosuke Osawa

Participation Coordinators

Adal D. Galván Castro
Carlos Martínez López

Administrative Assistant

Aurora García Sarrión

Web page: https://torroja.dmt.upm.es/causturb/

Meeting Venue:
Aula Magna, School of Aeronautics
Plaza Cardenal Cisneros 3, Ciudad Universitaria
28040 Madrid

Wifi options:
1) eduroam
2) Network: InvitadosUPM **(open your browser)**
User: causturb, **Password:**

Tuesday 3

8:30-9:00	Registration		
9:00-9:15	Welcome: J. Jiménez		
Chairperson: A. Lozano-Durán			
9:15-10:00	P. Koumoutsakos	Harvard U.	**Invited:** Multi-agent reinforcement learning in flow modelling and control
10:00-10:30	Coffee		
10:30-10:50	X. S. Liang, L. Wang, W. Li **(Remote)**	Fudan U.	Information flow and bottom-up causation in a quasi-geostrophic turbulence
10:50-11:10	M.P. Encinar, J. Jiménez	UP Madrid	Machine-aided discovery of significant regions in isotropic turbulence
11:10-11:30	X. Zhang, J. Jiménez **(Remote)**	Beihang U.	Causality in isotropic turbulence at low Reynolds number
11:30-11:50	Z. Hao, R. García-Mayoral	U. Cambridge	Inter-scale causality in near-wall turbulence
12:00-13:30	Lunch		
Chairperson: G. Boffetta			
13:30-13:50	G. Boga, E. Stalio, A. Cimarelli	U. Modena	Causality in turbulent entrainment of a passive scalar in free-shear flows
13:50-14:10	D. Lohse	U. Twente	Causality in Rayleigh-Bénard and Taylor-Couette turbulence
14:10-14:30	S. Brizzolara, M.E. Rosti, A. Mazzino M. Holzner	ETHz	Causality in immiscible Rayleigh-Taylor turbulence
14:30-14:50	D. Massaro, S. Rezaeiravesh, P. Schlatter	KTH	Causality-based algorithms for adaptive mesh refinement in turbulent flow simulations
14:50-15:20	Coffee		
Chairperson: M. Uhlmann			
15:20-15:40	E. López, R. Vinuesa, S. Le Clainche, A. Lozano-Durán, A. Srivastava	Illinois I. Tech.	Causality analysis of large-scale structures in urban flows
15:40-16:00	E. Kannadasan, C. Atkinson, J. Soria	Monash U.	Spectral analysis of the evolution of energy-containing eddies
16:00-16:20	K. Osawa, J. Jiménez	UP Madrid	Massive computational study of causal events in turbulent channel flow
16:20-16:40	J.E. Wesfreid, T. Liu, B. Semin, R. Godoy-Diana	ESPCI/CNRS	Dynamics of turbulent structures in Couette-Poiseuille flow
16:40-17:00	Y. Ling, A. Lozano-Durán	MIT	Comparison between interventional and observational causal inference in turbulence

Wednesday 4

Chairperson: G. Kawahara			
9:00-9:45	K. Taira, C-A. Yeh, K. Fukami	UCLA	**Invited:** Broadcasting Perturbations over Turbulence
9:45-10:15	Coffee		
10:15-10:35	H. Babaee	U. Pittsburgh	On-the-fly Reduced-Order Modeling of Turbulent Flow Response to High-Dimensional Forcing with Time-Dependent Bases
10:35-10:55	E. Ballouz, B. López-Doriga, S.T.M. Dawson, H.J. Bae	Caltech	Time-localized resolvent analysis for the study of causal relations in turbulent flows
10:55-11:15	Z. del Rosario, Ll. Jofre, G. Iaccarino	Stanford U.	Uncovering the link between dimensional analysis and causality
11:15-11:35	A. Vela-Martín, M. Avila	U. Bremen	Large-scale dynamics determines the predictability of extreme events in turbulence
11:35-11:55	A. Vela-Martín, M. Avila	U. Bremen	Causality in drop-turbulence interactions: identifying the driver of drop deformation and breakup
12:00-13:30	Lunch		
Chairperson: P. Koumoutsakos			
13:30-14:15	M. Rodwell	ECMWF	**Invited**: Butterflies in the atmosphere: Evaluating local divergence on the model attractor.
14:15-14:35	G. Boffetta, S. Musacchio	U. Torino	Predictability of homogeneous isotropic turbulence
14:35-14:55	C.J. Sear, S. Cowley	U. Cambridge	Inherent high-frequency instabilities developing from smooth noiseless initial conditions
14:55-15:25	Coffee		
15:25-15:45	M. Oberlack, S. Hoyas	TU Darmstadt	Cause and Effect in Turbulence - a Statistical Point of View
15:45-16:05	J. Westerweel, E.J. Grift M. Tummers (W. van de Water)	Delft U. Tech.	Variability of the flow around an impulsively started pitching blade
16:05-16:25	C. González-Hernández, Q. Yang, Y. Hwang	Imperial Col. London	Generalised quasilinear approximations of turbulent channel flow. Streamwise nonlinear energy transfer
16:25-17:30	**Discussion** Moderators: D. Lohse, A. Lozano-Durán		

21:00 Conference Dinner

Thursday 5

Chairperson: M. Avila			
9:00-9:45	G. Kawahara	Osaka U.	**Invited:** Invariant solutions and causality in turbulence
9:45-10:15	Coffee		
10:15-10:35	S. Motoki, G. Kawahara, M. Shimizu	Osaka U.	Ultimate heat transfer in coherent thermal convection
10:35-10:55	M. Nagata **(Remote)**	Kyoto U.	New class of solutions in plane Couette flow
10:55-11:15	M. Scherer, M. Uhlmann	Karlsruhe IT	Causality in sedimentary turbulent channel flows
11:15-11:35	M. Uhlmann, T. Pestana, M. Krayer, G. Kawahara	Karlsruhe IT	Investigating the interaction between turbulent flows and suspended particles with the aid of invariant solutions
11:35-11:55	E. Taschner, M. Beneitez, Y. Duguet, D.S. Henningson	U. Cambridge	Scaling and spatio-temporal constraints of the minimal seed in boundary-layer flows
12:00-13:30	Lunch		
Chairperson: J. Jiménez			
13:30-14:15	J. Runge **(Remote)**	DLR and TU Berlin	**Invited:** Causal inference, causal discovery, and machine learning
14:15-14:45	Coffee		
14:45-15:45	General discussion Moderators: G. Giaccarino, P.J. Schmid		
15:45-15:47	Closing remarks: J. Jiménez		

Abstracts

MULTI-AGENT REINFORCEMENT LEARNING IN FLOW MODELLING AND CONTROL

Petros Koumoutsakos
School of Engineering and Applied Sciences, Harvard University
E-mail: petros@seas.harvard.edu

What is the best way to learn fluid mechanics: by observing or by interacting with the flow field? Reinforcement Learning (RL) caters to the later approach for the modeling and control of fluid flows. Both problems can be cast in a similar formalism implying agents that provide either a closure or a control mechanism. Agents learn to optimize the long term consequences of their actions to the environment resulting in policies that map states to actions. We demonstrate how this can be a potent way of discovery of effective modeling and control strategies in turbulent flows. I will analyse success and failures of RL in collective swimming, navigation and closures for wall bounded flows. I will argue that while RL is a potent modality for discovery of (causal?) flow processes progress hinges on the proper incorporation of fluid mechanics knowledge in its algorithmic components.

INFORMATION FLOW AND BOTTOM-UP CAUSATION IN A QUASI-GEOSTROPHIC TURBULENCE

X. San Liang[1,2], Lipo Wang[3], and Weipeng Li[3]
[1]*Fudan University, Shanghai, China;*
[2] *Shanghai Qizhi (Andrew C. Yao) Institute, Shanghai, China;*
[3]*Shanghai Jiaotong University, Shanghai, China.*
E-mail: xsliang@fundan.edu.cn

A fundamental problem regarding the emergence of patterns in a fluid flow is how energy and information are exchanged across scales. While energy transfer has been extensively investigated, the latter, which is believed to be more fundamental since, in statistical physics, entropy may control the redistribution of energy, has been mostly overlooked. This latter transfer is what we nowadays call information transfer or information flow (IF). During the past few decades, IF has been put on a rigorous footing (beginning with [1]), with a bonus finding that causality actually can be derived from first principles[3], other than axiomatically proposed as an ansatz. A comprehensive study with generic systems has been fulfilled recently, with explicit formulas attained in closed forms[3]. The resulting metric of causality is invariant upon arbitrary nonlinear transformation, indicating that it is an intrinsic physical property[4]. The principle of nil causality, which every formalism seeks to verify in applications, turns out to be a theorem in this framework. In the linear sense, the maximum likelihood estimator of the metric is very concise, involving only the common statistics namely covariances. A corollary is that causation implies correlation, but not vice versa[2]. Problems such as causal graph reconstruction and self-loop identification are made easy[5].

The above formalism has been validated with benchmark systems like baker transformation, Hénon map, Kaplan-Yorke map, Rössler system[3], among others. It has also been applied to many real world problems in the diverse disciplines such as climate science, neuroscience, financial economics, etc. The recent remarkable success of El Niño Modoki predition[6], which has become a benchmark problem for the testing of AI algorithms, is such an example.

In this talk, we will present an application to the investigation of the formation of patterns out of an otherwise noisy quasi-geostrophic flow. By inverting a three-dimensional elliptic differential operator, the model is first converted into a low-dimensional dynamical system, where the components correspond to different time scales. The information exchange between the scales is then computed through ensemble prediction. Two cases are distinguished: The first concerns the emergence of coherent structures out of white noises, while the second has a basic flow in presence. It is found that in both cases the processes are dominated by a bottom-up causation, as collective patterns emerge out of independent entities (self-organization), but in the second case, top-down causation also plays a role at times when certain conditions are met.

Keywords: causality; information flow; multiscale interaction; self-organization; quasi-geostrophic turbulence

References

[1] Liang, X.S. and Kleeman, R. Information transfer between dynamical system components. *Phys. Rev. Lett.* **95**, 244101 (2005).
[2] Liang, X.S. Unravelling the cause-effect relation between time series. *Phys. Rev. E* **90**, 052150 (2014).
[3] Liang, X.S. Information flow and causality as rigorous notions *ab initio*. *Phys. Rev. E* **94**, 052201 (2016).
[4] Liang, X.S. Causation and information flow with respect to relative entropy. *Chaos* **28**, 075311 (2018).
[5] Liang, X.S. Normalized multivariate time series causality analysis and causal graph reconstruction. *Entropy* **23**, 679 (2021).
[6] Liang, X.S., Xu, F., Rong, Y., Zhang, R., Tang, X. and Zhang, F. El Niño Modoki can be mostly predicted more than 10 years ahead of time. *Nature Sci. Rep.* **11**, 17860 (2021).

MACHINE-AIDED DISCOVERY OF SIGNIFICANT REGIONS IN ISOTROPIC TURBULENCE

Miguel P. Encinar[1] and Javier Jiménez[1]
School of Aeronautics, Universidad Politécnica de Madrid, Madrid, Spain.
E-mail: mencinar@torroja.dmt.upm.es

Even if statistics of turbulent flow fields may be homogeneous, instantaneous snapshots of the flow are inhomogeneous at many scales. They exhibit regions where one or more observables of the flow, e.g. kinetic energy or enstrophy, are particularly intense, and stay so for a period of time. Turbulence researchers refer to these regions as coherent structures [7], and they have been a staple in turbulence analysis since their early observations [1]. Typically the relevance of some measurable quantity to the flow dynamics is inferred from the equations of motion (e.g. vorticity appears in the kinetic energy equation) and they are characterised by observing their distribution (following the example, intense vorticity is found to be organised in intense vortices that tend to cluster together [2]).

In this work, we attempt to study regions of the flow relevant to its dynamics, reversing the classical procedure sketched above. We take an approach similar to the one recently proposed by Jiménez [3, 4, 5], which seeks to discover features of the flow staying as free from human bias as possible. First, an initial condition is seeded with localised perturbations, and simulations are performed for each perturbed flow field, tracking the perturbation growth as a function of time. The perturbations used here zero either the local velocity fluctuations or the local vorticity within a region of a given size Δ. Some perturbations are found to grow up to 10^3 times more than others after one turnover, in terms of the global kinetic energy or enstrophy of the perturbation field. Because perturbations are local in space, the procedure classifies regions of the flow according to how much they grow when perturbed. The most 'reactive' regions are studied, showing that they tend to contain strong events, either strong vortices, strong velocity perturbations, or both. We study the top 5% of the structures that grow the most or the least, referring to them as significant or insignificant, respectively.

Large velocity perturbations ($\Delta > 60\eta$) grow or not based on the contribution of the region to the turbulent kinetic energy, whereas smaller ones ($\Delta < 60\eta$) do so based on the vorticity the local flow induces in the rest of the flow field. For the limiting size, $\Delta \approx 60\eta$, both features are equally important for perturbation growth and thus significant regions have more energy and enstrophy than insignificant ones. Figures (1b) and (1c) show the typical configuration of significant and insignificant regions of the flow at size 60η, hinting that the flow in significant regions is more 'complex'. The complexity of the flow is characterised using a box-counting algorithm [6], which allows us to estimate the fractal dimension of the three-dimensional distribution of enstrophy. Figure (1a) shows the estimated fractal dimension for the significant and insignificant sets, with fractal dimensions $D \approx 1.4$ and $D \approx 2.3$ respectively. This suggests that intense regions of vortex clusters are more sensitive to perturbations than the weaker vorticity layers found in insignificant regions.

This work is supported by the grant ERC-AdG-101018287, "CausT".

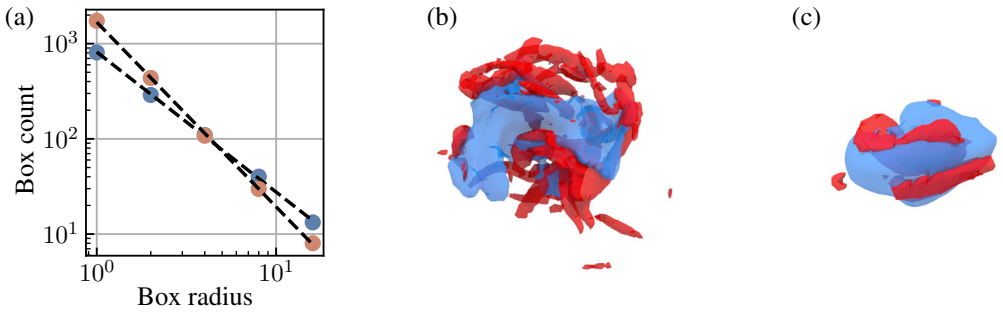

Figure 1. (a) Average box-counting for the significant (blue) and insignificant (orange) regions. The slopes are fitted to $D = 2.3$ (insignificant) and $D = 1.4$ (significant). (b,c) Example of the flow in one significant (a) and one insignificant (b) region. The red iso-surface denotes intense enstrophy and the blue surface, intense kinetic energy. Thresholds are chosen from a percolation analysis.

References

[1] G. L. Brown and A. Roshko. On density effects and large structure in turbulent mixing layers. *J. Fluid Mech.*, **64**:775–816, 7 1974.
[2] J. Jiménez, *et al.* The structure of intense vorticity in isotropic turbulence. *J. Fluid Mech.*, **255**:65–90, 10 1993.
[3] J Jiménez. Machine-aided turbulence theory. *Journal of Fluid Mechanics*, **854**:R1, 2018.
[4] J. Jiménez. Dipoles and streams in two-dimensional turbulence. *Journal of Fluid Mechanics*, **904**:A39, 2020.
[5] J. Jiménez. Monte carlo science. *J. Turbul.*, **21**(9-10):544–566, 2020.
[6] F. Moisy and J. Jiménez. Geometry and clustering of intense structures in isotropic turbulence. *J. Fluid Mech.*, **513**:111–122, 2004.
[7] S. K. Robinson. Coherent motions in the turbulent boundary layer. *Ann. Rev. Fluid Mech.*, **23**:601–639, 1991.

CAUSALITY IN ISOTROPIC TURBULENCE AT LOW REYNOLDS NUMBER

Xinxian Zhang[1] and Javier Jiménez[2]
[1]*School of Aeronautical Science and Engineering, Beihang University, PR China.*
E-mail: zhangxinxian@buaa.edu.cn
[2]*Aeronautics, Universidad Politécnica de Madrid, 28040 Madrid, Spain.*
E-mail: jjsendin@gmail.com

What kind of turbulent structures most affect the flow in homogeneous isotropic turbulence (HIT) at low Reynolds number? How do they affect it? Even though these questions have been discussed for years, they remain open. Here, we address whether causality analysis may provide us with new insights on them.

For our analysis, we perform a large number of three-dimensional direct numerical simulations of HIT in a 64^3 cubical grid, at Reynolds number $Re_\lambda \approx 50$. Following previous work in 2-D turbulence [1, 2], we modify small parts of the flow (cells) at $t = 0$, monitor the effect on the flow, and define as casually significant cells those whose modification leads to a large overall change in the flow at some later measurement time, $t = t_m$. Our goal is to first determine whether especially significant flow regions exist, and, second, whether they share some common characteristic. To do this, 65 basic initial turbulent flows are created, and each of them is divided into 10^3 cubical cells, about 12η on the side. The flow within each cell is modified in eight different ways (4 modifications of the vorticity field, and 4 of the velocity field), and the simulations are continued for one or two turnover times. Several definitions of 'significance' are used, based on the normalized L_2 and L_∞ norms of the velocity and vorticity difference between the modified and unmodified flows at $t = t_m$: i.e., $\|\Delta\boldsymbol{u}\|_2$, $\|\Delta\boldsymbol{u}\|_\infty$, $\|\Delta\boldsymbol{\omega}\|_2$, and $\|\Delta\boldsymbol{\omega}\|_\infty$. They all measure the importance of the original cell in determining the future behaviour of the flow as a whole. This is repeated for each cell and each kind of experimental modification, for a total of $65 \times 1000 \times 8 = 5.2 \times 10^5$ simulations. In addition, two normalizations are used for the significance: 'absolute significance', defined as in $\epsilon_a(L_2u) = \|\Delta\boldsymbol{u}\|_2/\|\boldsymbol{u}\|_2^{t=0}$, and 'relative significance', as in $\epsilon_r(L_2u) = \|\Delta\boldsymbol{u}\|_2/\|\Delta\boldsymbol{u}\|_2^{t=0}$. Norms without superscript are evaluated at $t = t_m$. The final step is to find which 'diagnostic' cell properties, defined as cell averages $\langle\bullet\rangle_c$ at $t = 0$, can best be used to predict whether cells will turn out to be significant or not.

Our results indicate that especially significant regions exist in HIT at low Reynolds number. Figure 1 shows the classification score of three different diagnostic quantities, where unity means 100% classification success, zero means 100% failure, and 0.5 is akin to a random guess. Figure 1(a), for a vorticity experiment, shows that the most sensitive cells are in that case those with initially high enstrophy, and that their effect peaks at about half a turnover time. Figure 1(b), for a velocity experiment, shows that the diagnostic quantity in this case is high initial kinetic energy. Note that these are not trivial results, such as that strong perturbations have strong effects, because the diagnostic ability applies to both absolute and relative significance, especially for velocity perturbations. In general, high enstrophy and high-energy cells do not coincide, suggesting two different types of significant flow configurations.

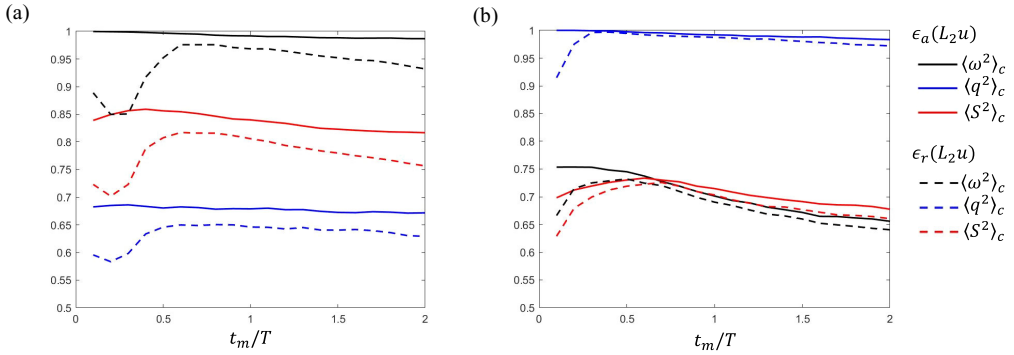

Figure 1. Score for the classification of cells as significant or insignificant, using three different diagnostic quantities, $\langle\omega^2\rangle_c$, $\langle q^2\rangle_c$, and $\langle S^2\rangle_c$. For perturbations (a) $\boldsymbol{\omega} \to 0$. (b) $\boldsymbol{u} \to 0$. Significant and insignificant regions are defined by the L_2 norm of the velocity difference, $\|\Delta\boldsymbol{u}\|_2$, both as 'absolute significance', $\epsilon_a(L_2u)$, or as 'relative significance', $\epsilon_r(L_2u)$.

References

[1] Jiménez J, "Machine-aided turbulence theory." *J. Fluid Mech.* **854**, R1(2018).
[2] Jiménez J, "Monte Carlo science." *J. Turbul.* **21**(9-10), 544-566 (2020).

INTER-SCALE CAUSALITY IN NEAR-WALL TURBULENCE

Zengrong Hao[1] and Ricardo García-Mayoral[2]
Department of Engineering, University of Cambridge, CB2 1PZ, UK.
E-mail: r.gmayoral@eng.cam.ac.uk

This work aims to map how information is transferred between different lengthscales through the momentum equations in near-wall turbulence, with a particular focus on streamwise and spanwise lengthscales. For this we use direct simulations in streamwise-spanwise-periodic turbulent channels. In this setup, the flow can be viewed as a dynamical system where the state space variables $\phi = \{u, w, v, p\}$ are the streamwise (x), spanwise (z) and wall-normal (y) velocities and the pressure, which depend on the x- and z-wavenumbers $\mathbf{k} = (k_x, k_z)$, y, and t. The evolution equations for ϕ are the Navier-Stokes equations plus the continuity equation, which can then be written as

$$F(\phi_{\mathbf{k},y,t}) = N(\psi_{\mathbf{k}',y,t}, \psi_{\mathbf{k}+\mathbf{k}',y,t}),$$

where F represents the linear part of the equations and N the nonlinear terms, which are responsible for the transfer of information from other lengthscales into lengthscale $\mathbf{k}$. The objective of this work is to quantify the relative importance of the different terms in N. The aim is to obtain results such as: w in wavelength λ_1 in combination with $\partial_z u$ in wavelength λ_2 play a significant role in the dynamics of u in wavelength λ_3, and so forth – note that, in turn, u in wavelength λ_3 and $\partial_z u$ in wavelength λ_2 do not appear combined in the momentum equation for w in wavelength λ_1. While intimately connected to triadic interactions, which are obtained from energy considerations, this analysis, relying instead on the momentum equations, aims to add a layer of directionality (i.e. causality) to the triple interactions.

CAUSALITY IN TURBULENT ENTRAINMENT OF A PASSIVE SCALAR IN FREE-SHEAR FLOWS

G. Boga, E. Stalio and A. Cimarelli
DIEF, University of Modena and Reggio Emilia, 41125 Modena, Italy.
E-mail: gabriele.boga@unimore.it; enrico.stalio@unimore.it; andrea.cimarelli@unimore.it

Numerical experiments on the turbulent entrainment and mixing of scalars in an incompressible temporal planar jet flow [1] have been performed [2]. These simulations are based on a scale decomposition of the velocity field, thus allowing the establishment from a dynamic point of view of the evolution of different scalar fields under the separate action of large-scale coherent motions and small-scale fluctuations, see Figure 1(a). This is the main novelty that differentiates the present work from other studies dealing with the analysis of flow realization snapshots, e.g. [3], [4] and [5]. The turbulent spectrum can be split into active and inactive flow structures. The large-scale engulfment phenomena actively prescribe the mixing velocity by amplifying inertial fluxes and by setting the area and the fluctuating geometry of the scalar interface [6]. On the contrary, small-scale isotropic nibbling phenomena are essentially inactive in the mixing process. It is found that the inertial mechanisms initiate the process of entrainment at large scales to be finally processed by scalar diffusion at the molecular level. This last stage does not prescribe the amount of mixing but adapts itself to the conditions imposed by the coherent anisotropic motion at large scales. The effectiveness of the large-scale motions in prescribing a large scalar interface area and in maintaining steep scalar gradients resulted in a faster growth in entrained volume with respect to the one induced by small-scale fluctuations, as shown in Figure 1(b). Additionally, the presence of protruding bulges on the scalar interface generated by large-scale motions resulted in a faster growth of the jet width with respect to the small-scale case, as can be seen in the inset of Figure 1(b). The present results may have strong repercussions for the theoretical approach to scalar mixing, as anticipated here by simple heuristic arguments which are shown able to reveal the rich dynamics of the process. Interesting repercussion are also envisaged for turbulence closures, in particular for large-eddy simulation approaches where only the large scales of the velocity field are resolved.

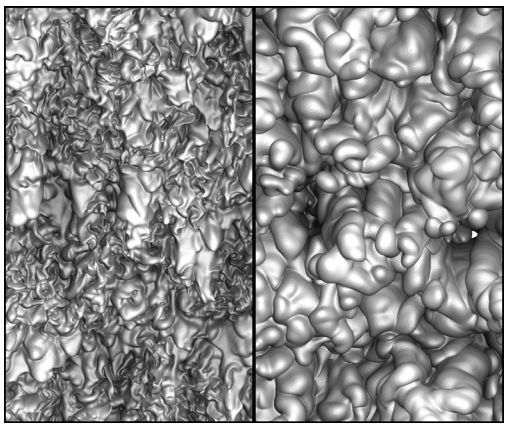

(a)

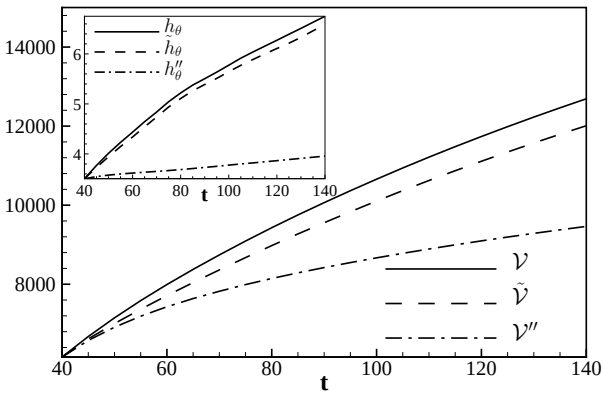

(b)

Figure 1. (a) Instantaneous scalar interface ($\theta_{th} = 0.02\Theta_{cl}$) in the two experiments at time $t = 120$: small-scale driven scalar field (left) and large-scale driven scalar field (right). (b) Temporal evolution of the entrained volume $\mathcal{V}$ and of the position of the interface h_θ (inset) for the scalar field driven by the unfiltered velocity field $\mathcal{V}$ and h_θ (solid line), by the large-scale velocity field $\tilde{\mathcal{V}}$ and $\tilde{h_\theta}$ (dashed line) and by the small-scale velocity field $\mathcal{V}''$ and h''_θ (dashed-dotted line).

References

[1] Van Reeuwijk, M., & Holzner, M. 2014. The turbulence boundary of a temporal jet. *J. Fluid Mech.*, **739**, 254-275.
[2] Cimarelli, A., & Boga, G. 2021. Numerical experiments on turbulent entrainment and mixing of scalars. *J. Fluid Mech.* **927**, A 34.
[3] da Silva, C.B. & Pereira, J.C. 2008. Invariants of the velocity-gradient, rate-of-strain, and rate-of-rotation tensors across the turbulent/nonturbulent interface in jets. *Phys. Fluids*, **20**, 055101.
[4] Watanabe, T., Sakai, Y., Nagata, K., Ito, Y. & Hayase, T. 2015 Turbulent mixing of passive scalar near turbulent and non-turbulent interface in mixing layers. *Phys. Fluids* **27** (8), 085109.
[5] Westerweel, J., Fukushima, C., Pedersen, J.M. & Hunt, J.C.R. 2005 Mechanics of the turbulent-nonturbulent interface of a jet. *Phys. Rev. Lett.* **95** (17), 174501.
[6] Sreenivasan K. R., Ramshankar R. & Meneveau C. 1989. Mixing, entrainment and fractal dimensions of surfaces in turbulent flows. *Proc. R. Soc. Lond.* A **421**, 79–108.

CAUSALITY IN RAYLEIGH-BÉNARD AND TAYLOR–COUETTE TURBULENCE

Detlef Lohse
Physics of Fluids, University of Twente

The Rayleigh-Bénard (RB) and Taylor-Couette (TC) systems have always been the drosophila of physics of fluids, with various concepts in fluid dynamics such as stability, pattern formation, transition to turbulence, transitions in the boundary layer, or transport properties being tested with these well-defined flows with well-known underlying dynamical equations and boundary conditions. We think that RB and TC are excellent playgrounds to also test new ideas on causality in turbulence and to better understand what one can learn when asking questions on observed effects and underlying causes.

Examples are about the connection between the number of observed large-scale rolls in these systems and the aspect ratio, about flow reversals and how they depend on the control parameters, about multiple co-existing turbulent states, and about the effects of plate roughness on the turbulent transport properties of the flow.

I will try to elucidate the questions formulated in the flyer of the workshop in the context of these examples, which are all current research questions in the field of RB and TC turbulence.

CAUSALITY IN IMMISCIBLE RAYLEIGH-TAYLOR TURBULENCE

Stefano Brizzolara[1,2], Marco Edoardo Rosti[3], Andrea Mazzino [4] and Markus Holzner[2,5]
[1] *Institute of Environmental Engineering, ETH Zurich, CH-8039 Zurich, Switzerland*
[2] *Swiss Federal Institute of Forest, Snow and Landscape Research WSL, 8903 Birmensdorf, Switzerland*
[3] *Complex Fluids and Flows Unit, Okinawa Institute of Science and Technology Graduate University, 1919-1 Tancha, Onna-son, Okinawa 904-0495, Japan*
[4] *DICCA, University of Genova and INFN, Genova Section, Via Montallegro 1, 16145, Genova, Italy*
[5] *Swiss Federal Institute of Aquatic Science and Technology Eawag, 8600 Dübendorf, Switzerland*
E-mail: brizzolara@ifu.baug.ethz.ch

Rayleigh-Taylor instability (RTI) originates at the interface between a layer of heavier and lighter fluid in the presence of an acceleration. At late times, the RTI evolves in a self-similar turbulent state, sustained by the continuous conversion of potential into kinetic energy [1]. RT turbulence phenomenology entails that, by balancing kinetic and potential energy, one obtains a quadratic scaling in time of the mixing zone, i.e. $h(t) = \alpha A g t^2$, where A is the Atwood number (the ratio between the density increment and the mean density) and g the gravitational acceleration. α is a constant coefficient that represents the efficiency at which the potential energy is converted into kinetic energy [2].

When the two phases are immiscible, the interfacial tension does not allow a complete mixing of the fluids. In fact, the turbulence fragments one fluid into the other, generating an emulsion-like state where the characteristic droplet size (the Hinze scale) decreases in time, resulting from a balance between the kinetic and the interfacial energy density. In our work we study the properties of this emulsion-like state, and in particular the causal relation between the self-similar turbulence state and the emulsion properties represented by the Hinze scale, the interface surface area and the velocity pair-correlation function.

To this purpose, we compare physical experiments (Figure 1) and direct numerical simulations to a self-consistent phenomenological theory designed to describe the underlying phenomenon [3]. With their phenomenology, Chertkov and co-authors speculate that the Hinze scale passively adapts to the large scales of the flow. The bubble generation is therefore considered to be a consequence of the large-scales, and is believed to not produce any back-reaction on the global features of the mixing.

Our experiments and simulations reveal that the convergence of the α coefficient is slowed down by the interfacial tension; more in detail, the stronger the interfacial tension, the later the turbulence reaches its self-similar state for which α is constant. Nevertheless, whether this correlation implies causality is not yet clear. Indeed, the delay in reaching the self-similar state could be due to the bubbles at the Hinze scale, that are originated not only from the interfacial tension but also from the kinetic energy cascade. If the bubbles delay the self-similar state, this means that they back-react on the large scales for some time. If this is the case, the assumption under which the emulsion properties can be considered a consequence of the large scale evolution breaks down, and a new phenomenology has to be derived.

To clarify the relation between the large scales and the bubble production, we aim to control independently each of the governing parameters. That is, we will keep the Hinze scale evolution unchanged and modify the interfacial tension at the same time. This can be done by decreasing the Atwood number and the interfacial tension together. We expect that this will provide a clear picture on the causal relations underpinning the evolution of immiscible RT turbulence that is potentially relevant for a broader class of turbulent flows with unsteady forcing mechanisms.

Figure 1. Snapshots of a laser induced fluorescence RT turbulence experiment (time interval between the images: $0.1\,s$, scale bar: $14\,mm$). The experiment is conducted using hexane as light fluid and a mixture of water and glycerol (37% in weight) as heavy fluid.

References

[1] Boffetta, G. and Mazzino A. "Incompressible rayleigh–taylor turbulence." Annual Review of Fluid Mechanics 49 (2017): 119-143.
[2] Chertkov, M. "Phenomenology of rayleigh-taylor turbulence." PRL 91.11 (2003): 115001.
[3] Chertkov, M., Kolokolov, I. and Lebedev, V. "Effects of surface tension on immiscible Rayleigh-Taylor turbulence." PRE 71.5 (2005): 055301.

CAUSALITY-BASED ALGORITHMS FOR ADAPTIVE MESH REFINEMENT IN TURBULENT FLOW SIMULATIONS

Daniele Massaro and Saleh Rezaeiravesh and Philipp Schlatter
SimEx/FLOW, Engineering Mechanics, KTH Royal Institute of Technology, Stockholm, Sweden.
E-mail: dmassaro@kth.se

Computer infrastructures allow studying turbulent flows in more complicated geometries and at higher Reynolds numbers. By performing direct numerical simulations (DNS) all the spatial and temporal turbulent scales and associated dynamics may be captured. Nevertheless, the chaotic nature of the dynamical system does not allow to easily identify the relationship between different variables required for a complete understanding of the flow dynamics. In particular, such a relationship between the signals of different quantities can be inferred through, for instance, sensitivity, correlation, and causality analyses. Despite its simplicity, correlation-based inference is incapable of addressing the directionality of information. To overcome this deficiency, information theory provides alternative causality measures, such as information flow [1] and transfer entropy [2].

In the present study, we propose to compute the causality between the quantities of interest (QoIs) and flow variables, exploiting the acquired information to drive an Adaptive Mesh Refinement (AMR) algorithm. The resulting algorithm will be compared to the case of using information based on correlation and (local) sensitivity analyses. In a first step, for the two-dimensional flow around a circular cylinder at $Re = 200$, the transfer entropy between the velocity magnitude and a given quantity of interest, *i.e.* the cylinder drag, is computed and analysed.

The AMR technique aims at automatically designing a mesh, controlling the error and thus ensuring a significant computational saving. It becomes fundamental when the flow solution is not a-priori known. The main ingredients are error measurement and refinement strategy. In the open-source spectral-element code Nek5000 [3] the h-refinement is implemented which consists of the isotropic splitting the element when a certain criterion is satisfied. Regarding error evaluation, we have been using the spectral error indicator (SEI), which is a local measure of the quadrature and truncation errors, and the adjoint error estimator (AEE), a goal-oriented and dual-weighted residuals estimator. Unfortunately, the adjoint linear operator suffers from exponential sensitivity to any small perturbations, due to the chaotic nature of turbulent flows. In the literature, several methods have been proposed to remedy this, *e.g.* ensembles, shadowing or filtering, but no practical solution has been found yet. As a novel alternative, we propose an error estimator based on transfer entropy for identifying the regions which are causally related to our QoI. Moreover, considering some cases where SEI and AEE have been already applied, see [4, 5], a thorough comparison between the performance of different error indicators is possible and allows assessing the benefits of causality.

Bearing in mind this, we aim to address some fundamental questions as: is the casual inference, here measured through transfer entropy, really different from correlation? How is sensitivity analysis related to these? The answer to these questions is not only important for AMR, but also for relevant data-driven methods (e.g. optimization) of turbulent flows.

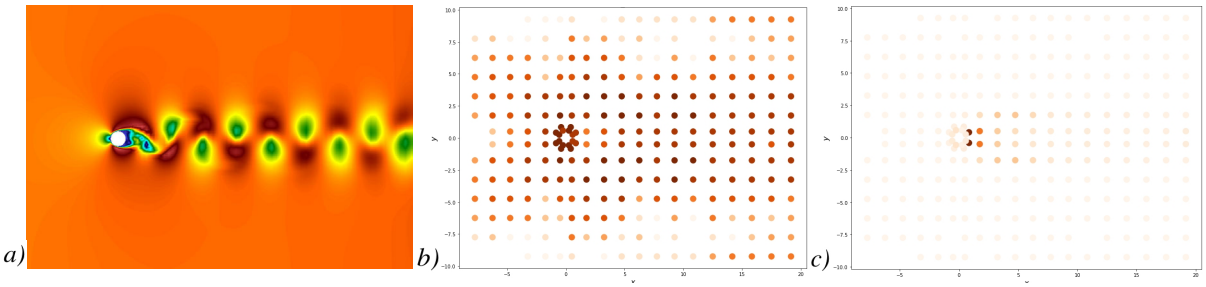

Figure 1. *a)* The instantaneous velocity magnitude for the flow around a circular cylinder at $Re = 200$. *b)* For each spectral element the time-averaged transfer entropy between the velocity magnitude and the cylinder drag (middle). *c)* Spectral error indicator averaged in time.

References

[1] Liang, X. S., and Kleeman, R. Information transfer between dynamical system components, *Phys. Rev. Lett.* **95**, (2006).
[2] Schreiber, T. Measuring information transfer. *Phys. Rev. Lett.* **85**, (2000).
[3] Fischer, P. F. and Lottes, J. W. and Kerkemeier, S. G. *Nek5000 Web page* (2008).
[4] Offermans, N. and Peplinski, A. and Marin, O. and Schlatter, P. Adaptive mesh refinement for steady flows in Nek5000. *Comput. Fluids* **197**, (2020).
[5] Offermans, N. and Massaro, D. and Peplinski, A. and Schlatter, P. Error-driven adaptive mesh refinement for unsteady turbulent flows in spectral-element simulations. *Comput. Fluids*, (submitted,2022).

CAUSALITY ANALYSIS OF LARGE-SCALE STRUCTURES IN URBAN FLOWS

Esteban Lopez[1†], Ricardo Vinuesa[2], Soledad Le Clainche[3], Adrián Lozano-Durán[4], Ankit Srivastava[1]
[1] *Dept. Mechanical, Materials, and Aerospace Engineering, Illinois Institute of Technology, Chicago, IL, 60616, USA*
[2] *FLOW, KTH Royal Institute of Technology, SE-100 44 Stockholm, Sweden*
[3] *School of Aerospace Engineering, Universidad Politécnica de Madrid, E-28040, Spain*
[4] *Department of Aeronautics and Astronautics, Massachusetts Institute of Technology, Cambridge, MA, 02139, USA*
[†] *E-mail: elopez8@hawk.iit.edu*

The aim of this work is to analyze the formation mechanisms of large-scale coherent structures in urban fluid flows, with focus on the so-called arch vortex. As shown in Figure 1 (left), this vortex is formed on the leeward side of wall-mounted obstacles, and this structure has an important impact on the transport of pollutants in urban areas. To this end, we assess causal relations between different proper-orthogonal-decomposition (POD) modes obtained from well-resolved large-eddy simulation (LES) data (slightly coarser than direct numerical simulation) of a number of urban configurations similar to that shown in Figure 1 (left). The causal relations are identified by conditional transfer entropy, which is an information-theory quantity which estimates the amount of information contained in the past of one variable about another, and as such offers a value indicating the predictive power available in the history of such variables. When applied to kinematic systems, transfer entropy reveals underlying dynamics driving different entities of the system, differentiating between causes and effects for each variable. This allows for an understanding of the origins of different phenomena in the flow, with the aim of identifying the modes responsible for the formation of the arch vortex. A preliminary study has been carried out to determine the causal relations present in the nine-equation model of near-wall turbulence developed by Moehlis *et al.* [1]. The aim of this is to verify the ability of the proposed method to identify causal interactions we expect to see a-priori. As shown in Figure 1 (right), some of the most prominent causal relations are analogous to those reported by Lozano-Durán *et al.* [2] in turbulent channel flow, namely: Mode 2 $\leftrightarrow$ Mode 4 (mean-flow instability in the spanwise direction); Mode 2 $\rightarrow$ Mode 6 and Mode 2 $\rightarrow$ Mode 9 (lift-up mechanism); Mode 6 $\rightarrow$ Mode 4 (roll generation). The complete contribution will contain an analogous analysis on the dominant POD modes of various urban environments, with the goal of shedding light into the mechanisms of pollutant transport in cities.

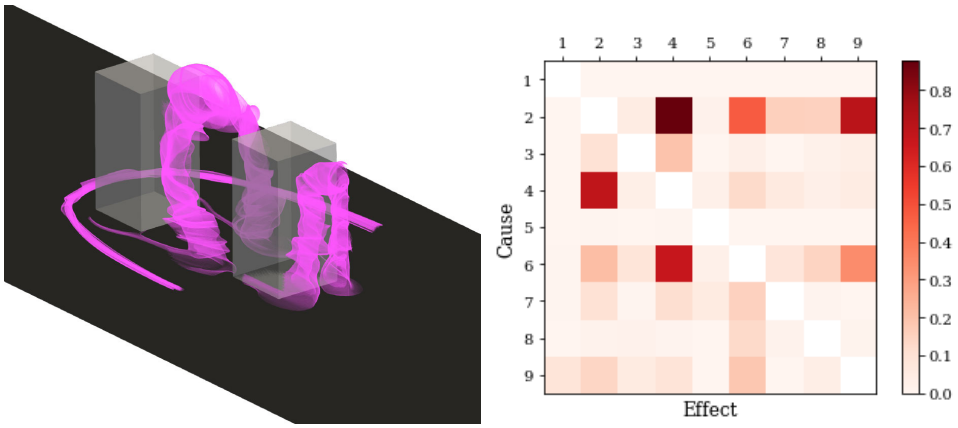

Figure 1. (Left) Streamlines in a simplified urban flow illustrating the arch and horseshoe vortices; flow from left to right. (Right) Causality analysis performed on the model by Moehlis *et al.* [1].

References

[1] J. Moehlis, H. Faisst, and B. Eckhardt, "A low-dimensional model for turbulent shear flows," *New J. Phys.*, vol. 6, p. 56, 2004.
[2] A. Lozano-Durán, H. J. Bae, and M. P. Encinar, "Causality of energy-containing eddies in wall turbulence," *J. Fluid Mech.*, vol. 882, p. A2, 2020.

SPECTRAL ANALYSIS OF THE EVOLUTION OF ENERGY-CONTAINING EDDIES

Ezhilsabareesh Kannadasan[1], Callum Atkinson[1] and Julio Soria[1]
Laboratory for Turbulence Research in Aerospace and Combustion (LTRAC),
Department of Mechanical and Aerospace Engineering,
Monash University,
Melbourne, Victoria 3800, Australia
E-mail: ezhilsabareesh.kannadasan@monash.edu.au

Energy-containing eddies are the elementary structures that carry most of the kinetic energy and momentum in wall-bounded turbulence. These eddies follow a self-sustaining cycle and can be structured in a hierarchical form attached to the wall. In this paper, the packets of energy-containing eddies are artificially quenched at the inlet of a turbulent channel flow direct numerical simulation (DNS), and the spatial evolution of the energy of the eddies is studied. The velocity fields from streamwise periodic channel flow (PCH-DNS) at Re_τ = *550* are filtered and used as the inlet velocity field for a channel flow DNS with inlet-outflow boundary conditions (IOCH-DNS). The turbulent transport spectra (Figure 1a) suggest that ridge λ_z = *3y* distinguishes the energy-containing eddies and the eddies involved in the energy cascade. The turbulent fluctuations and energy below the ridge λ_z = *3y* are removed, and only the eddies involved in the energy cascade are fed into IOCH-DNS at every time step. The mean velocity and fluctuating velocity profiles of IOCH-DNS are shown in Figure 1b, at x = *3h*, the mean velocity profile is distorted, and the streamwise fluctuation is evolved by extracting energy from the mean flow. The streamwise length of $24h$ is required to recover the turbulent fluctuations and energy when the energy-containing motions are removed at the inlet. At x = *24h*, the fluctuating velocity profiles are in good agreement with the PCH-DNS in the near-wall region, whereas, in the regions far from the wall ($y^+ > 150$) the fluctuations are damped. The pre-multiplied spanwise energy spectra of the streamwise velocity ($k_z\phi_{uu}$) of PCH-DNS are aligned along the ridge $\lambda_z = 10y$. In IOCH-DNS, as the flow evolves, energy starts to recover in the near-wall region ($y^+ \approx 10 \sim 15$) at a spanwise wavelength of $\lambda_z^+ \approx 100$, equal to the spanwise spacing of near-wall streaks, which indicates that the formation of near-wall streaks is the primary process in the recovery of energy-containing motions.

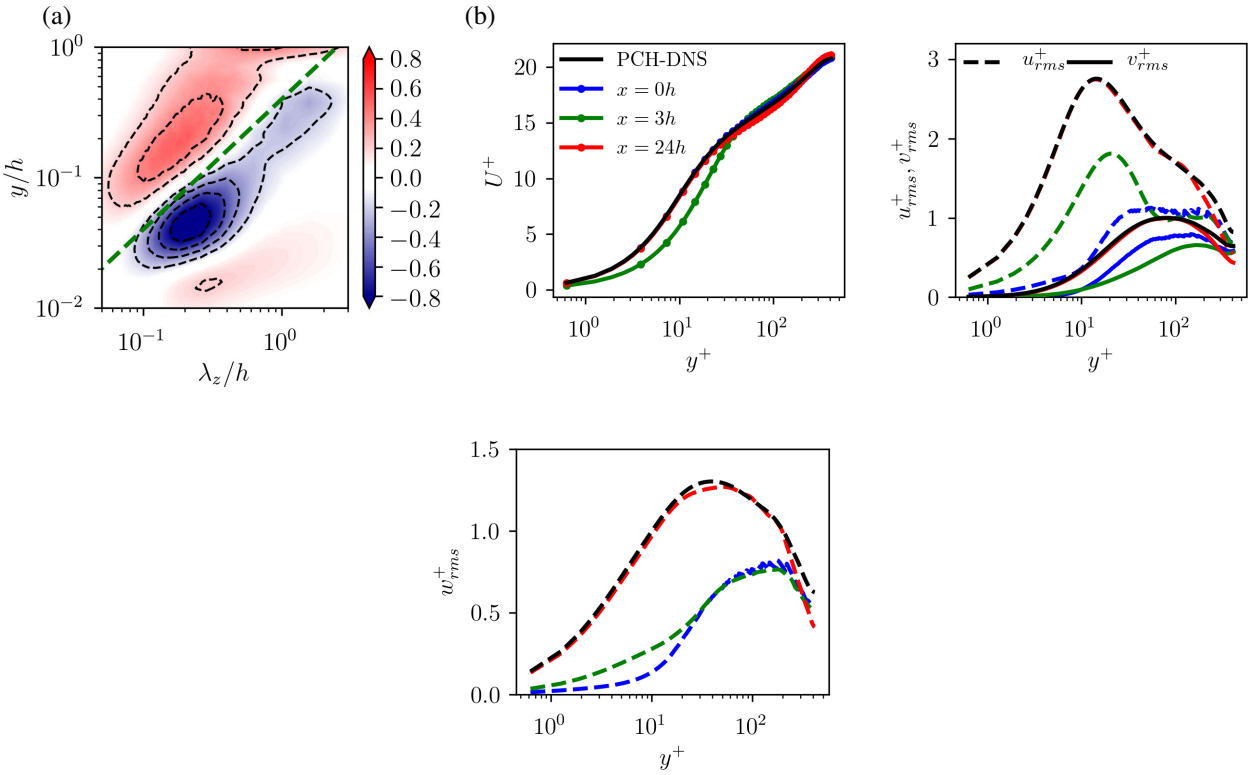

Figure 1. (a) The pre-multiplied spanwise spectra of turbulent transport ($k_z^+ y^+ \hat{T}^+_{\text{turb}}$) of PCH-DNS at $Re_\tau = 550$. Dashed green line is at $\lambda_z = 3y$, (b) Mean velocity profile and Root-mean-squared fluctuating velocity profiles at $Re_\tau = 550$. Here, black line, PCH-DNS; blue line, IOCH-DNS at x = *0h*; green line, IOCH-DNS at x = *3h*; red line, IOCH-DNS at x = *24h*.

MASSIVE COMPUTATIONAL STUDY OF CAUSAL EVENTS IN TURBULENT CHANNEL FLOW

Kosuke Osawa & Javier Jiménez
School of Aeronautics, Universidad Politécnica de Madrid, 28040 Madrid, Spain.
E-mail: kosawa@torroja.dmt.upm.es

Causally important events are studied in turbulent channel flow by seeing the effect of intervening init. The methodology follows the causal analysis of 2D HIT by Jiménez [1]. The basic idea is to perturb a small part (hereafter "cell") of the flow, and measure how much the development of the flow changes from the original, to know the causal significance of the perturbed cell. This experiment is repeated many times, and common flow features of causally significant or irrelevant cells are elucidated using large data ensembles. In this study, we perform a total of 29520 direct numerical simulations of turbulent open channel flow at $Re_\tau = 609$. The domain size is $l_x \times l_y \times l_z = \pi h \times h \times \pi h$, where x, y and z are the streamwise, wall-normal and spanwise directions, respectively, and h is the channel height. The initial perturbation is to remove the velocity fluctuations in the cell, implemented by overwriting the velocity in the cell with its $x-z$ mean, and imposing continuity after the modification. Cells are cubes of size of $l^+_{cell} = 25, 50, 100$ and 150, where the superscript $+$ denotes wall units. Because the flow is inhomogeneous in y, the central height of the cell, y_{cell}, is also an important parameter, and is varied from $l_{cell}/2$ (attached to the wall) to 300 wall units. Causal significance is either measured by the squared norm of the velocity difference between the perturbed and original flows, $\varepsilon_{\boldsymbol{u}} = ||\boldsymbol{u}_{per} - \boldsymbol{u}_{org}||^2$, or by its relative growth $\varepsilon_{\boldsymbol{u}}(t)/\varepsilon_{\boldsymbol{u}}(0)$.

Causal features change a lot depending on whether the causal significance is measured by the absolute magnitude of the difference, $\varepsilon_{\boldsymbol{u}}$, or by its relative growth. When the magnitude is used, cells with an initially larger perturbation tend to be more causally significant. This result is robust to the evaluation time, to l_{cell} and to y_{cell}. On the other hand, when the growth is used, the causally significant cells depend on the time and on y_{cell}. At the time, t_{sig}, at which the causal significance of the different cells diverges the most, significant cells tend to be in sweeps, whereas irrelevant ones tend to be in ejections. Figure 1 shows $\varepsilon_{\boldsymbol{u}}$ averaged over $x-z$ for: (a) significant cells, and (b) irrelevant ones. Generally, the perturbation initially spreads both up and down, but only grows substantially after it reaches the wall. As characterized by the peak height of $\varepsilon_{\boldsymbol{u}}$ (bold line), the perturbation of the significant cells move down to the wall faster than the irrelevant ones. This suggests that sweeps tend to be more causally significant than ejections because they carry the perturbation faster to the wall, where it develops due to the higher shear. The time t_{sig} is found to be roughly proportional to y_{cell}, supporting the idea that the perturbation propagation toward the wall decides its causal significance.

Funded by the Caust grant ERC AdG-101018287.

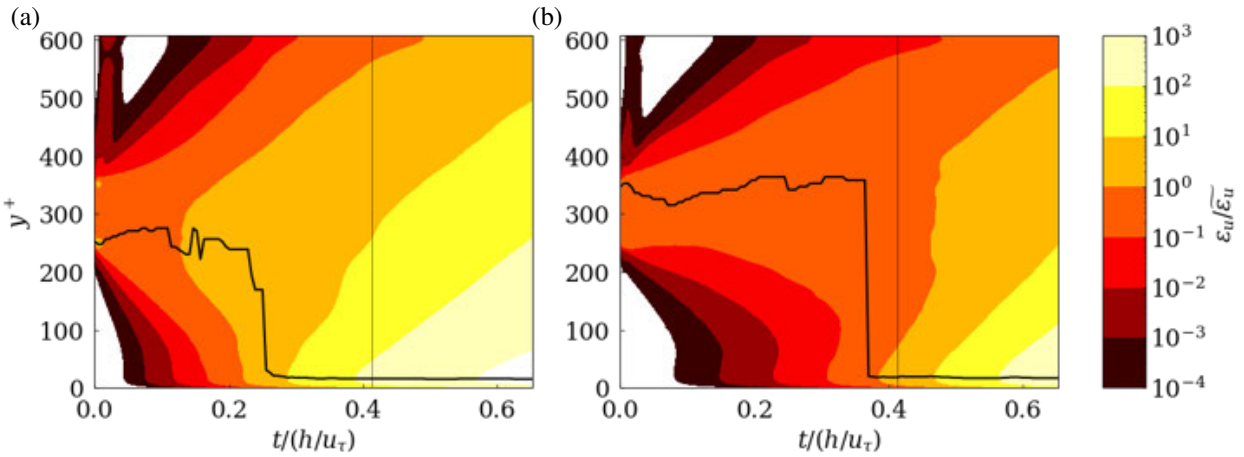

Figure 1. Temporal and wall-normal development of $\varepsilon_{\boldsymbol{u}}$, averaged over $x-z$. (a) Conditioned to causally significant perturbations. (b) Causally irrelevant. Causal significance defined by relative growth, and normalized by the initial $x-y-z$ mean value of all samples. Vertical line: t_{sig}. Bold line: Peak height of $\varepsilon_{\boldsymbol{u}}$. $l^+_{cell} = 100$, $y^+_{cell} = 300$.

References

[1] Jiménez, J, Computers and turbulence. *Europ. J. Mech. B: Fluids* **79**, 1–11 (2019).

DYNAMICS OF TURBULENT STRUCTURES IN COUETTE-POISEUILLE FLOW

José Eduardo Wesfreid, Tao Liu, Benoit Semin and Ramiro Godoy-Diana
Laboratoire PMMH (CNRS, ESPCI, Sorbonne Université, Université Paris Cité), 7 quai Saint-Bernard, 75005 Paris, France.
E-mail: wesfreid@pmmh.espci.fr

We carry out experiments in a plane Couette-Poiseuille channel (fig.1). The streaks and rolls are quantified respectively by the streamwise velocity u_x and the spanwise velocity u_z, measured using Particule Image Velocimetry (PIV).

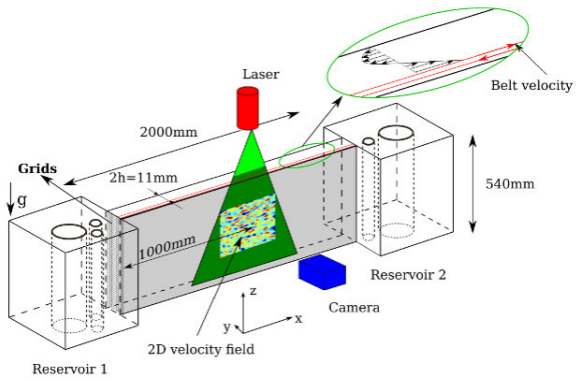

Figure 1. Couette-Poiseuille channel

We study the decay of turbulence using a 'quench' protocol, i.e. an abrupt decrease of the Reynolds number Re from a fully turbulent state to a laminar regime[1].
We show that the rolls decay faster than the streaks. The streaks have two decay stages in the decay process. During the first stage of the decay, the remaining rolls slow down the decay of the streaks. This is consistent with the lift-up effect, i.e. the formation of streaks by linear advection of the rolls.
We also study the effect of the noise, which is the external disturbance generated by the belt driving cylinder, on the transient decay and the permanent regime. The decay dynamics is independent of the noise level. The noise shifts the apparent critical onset of transition. We use the susceptibility of u_z in the permanent regime to quantify the noise intensity.
We present very recent results about the study the waviness of streaks using vortex generators to induce unstable wavy streaks. The evolution of the streaks becoming wavy from a straight state is characterized using stereoscopic PIV. We apply a spatial filter to separate the straight part and the wavy part of the flow (fig.2). Our experimental results show how the appearance of the spanwise velocity and the wall-normal velocity is correlated to the increase of the waviness of the streaks, as expected from self-sustaining models and give quantitative support to this relation.

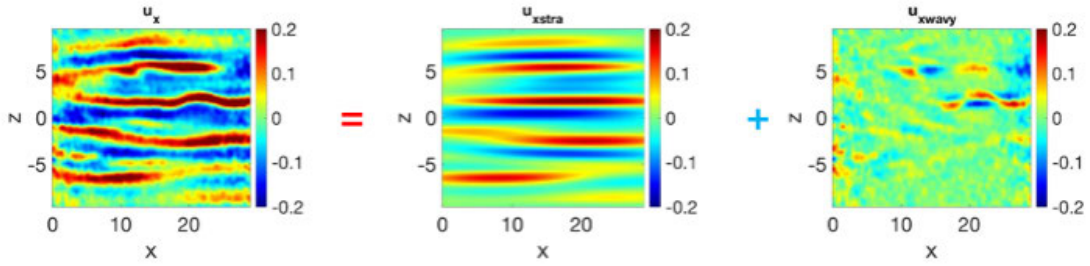

Figure 2. Decomposition of small scale streamwise velocity into straight and wavy components

References

[1] Liu, T., Semin, B., Klotz, L., Godoy-Diana, R., Wesfreid, J. E. and Mullin, T. Decay of streaks and rolls in plane Couette-Poiseuille flow, *J. Fluid Mech.* **915**, A65 (2021).

COMPARISON BETWEEN INTERVENTIONAL AND OBSERVATIONAL CAUSAL INFERENCE IN WALL TURBULENCE

Yuenong Ling[1] and Adrián Lozano-Durán[2]
Department of Aeronautics and Astronautics, Massachusetts Institute of Technology, Cambridge, MA 02139, USA.
E-mail: lingyn@mit.edu

Wall-bounded turbulent flows are ubiquitous in nature. Understanding the causality behind phenomena we observe in turbulence is essential for the modelling and control of industrial flows. Causal inference of scientific phenomena can be roughly categorized as interventional or observational [1]. Interventional studies rely on modifying the system conditions and assessing the consequences. They are often used for practical purposes due to the intuitive connection of cause and effect they portray [2]. However, in large complex systems such as turbulent flows, interventions are usually impossible in experimental setups and prohibitively expensive in numerical studies. Observational causal inference, conversely, only requires the time history of the flow and is more economical both computationally and experimentally. Nevertheless, the methods to evaluate observational causality are neither well-defined nor straightforward. To date, meaningful metrics to capture the causal relations between quantities remain to be established. In this paper, we study the causal interactions between energy-containing eddies in the buffer layer of a turbulent channel flow. The domain chosen for the channel as shown in figure 1(a) is a minimal box, which is sufficient to isolate the relevant dynamical structures [3]. For the interventional study, we examine the causality by freezing in time one of the Fourier mode coefficients in the buffer layer and observe its impact on other quantities. For the observational study, the time signal of the Fourier mode coefficients is extracted and the information flux proposed in [4] and illustrated in figure 1(b) is computed to find the causal interactions between different modes. The results and procedures of both studies are compared. Finally, the possibility of replacing interventional causal inference with its observational counterpart is discussed.

Funded by National Science Foundation under Grant 032707-00001.

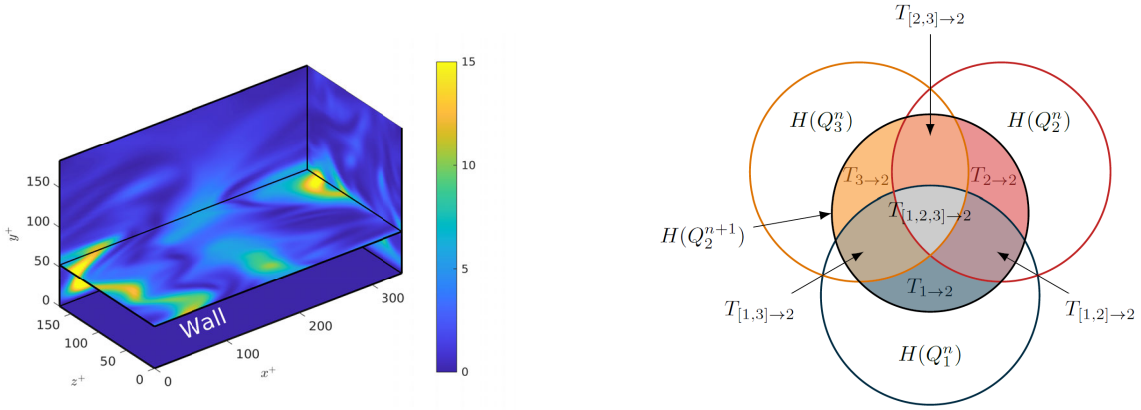

(a) (b)

Figure 1. (a) Turbulent kinetic energy in the buffer layer. (b) Schematic of information flux.

References

[1] Jiménez, J. Monte Carlo science. *Journal of Turbulence* **21.9-10**, 544-566 (2020).
[2] Pearl, J. Causality. Cambridge university press (2009).
[3] Jiménez, J. and Moin, P. The minimal flow unit in near-wall turbulence. *Journal of Fluid Mechanics*, **225**, 213-240 (1991).
[4] Lozano-Durán, A. and Arranz, G. Information-theoretic formulation of dynamical systems: causality, modeling, and control. *arXiv preprint* arXiv:**2111.09484.** (2021).

BROADCASTING PERTURBATIONS OVER TURBULENCE

Kunihiko Taira[1], Chi-An Yeh[2], and Kai Fukami[1]
[1]*Department of Mechanical and Aerospace Engineering, University of California, Los Angeles, CA, USA*
[2]*Department of Mechanical and Aerospace Engineering, North Carolina State University, Raleigh, NC, USA*
E-mail: ktaira@seas.ucla.edu

Disease transmission over human networks and information dissemination over social networks have become important areas of studies with significant societal impacts. The studies of these phenomena are founded on network science [1], which combines graph theory, dynamical systems, and data science. Taking inspirations from network-based analysis [2], we examine perturbation dynamics for turbulent flow networks. In this talk, we present the vortical network broadcast analysis for time-varying turbulent flows to identify the optimal flow modification strategy.

Network science specializes in analyzing, modeling, and controlling interaction dynamics over a collection of elements. Turbulent flow analysis is a key candidate to benefit from network science, because turbulence is influenced by the rich interactions amongst a large number of vortices present over a range of scales. In fact, we can study such vortical interactions by quantifying the induced velocity generated by the vortical structures [3]. Through the network-based analysis tools, we are able to extract dominant interactions present in turbulence and model its dynamics [4]. Of particular interest in this talk is the use of time-varying vortical networks to quantify time-dependent turbulent base flows. We quantify how perturbations added to turbulence can influence the overall perturbation dynamics using the network broadcast analysis [5]. This approach reveals the most amplified disturbances broadcast over the time-evolving turbulence network. We show that the broadcast analysis shares similarities with resolvent analysis [6, 7] in its formulation but for non-harmonic dynamics.

We demonstrate the utility of the network broadcast analysis to identify flow structures that can optimally modify turbulent flows for the examples of two-dimensional isotropic turbulence and separated turbulent flow over an airfoil. The results from these examples suggest that the present formulation holds promise in guiding time-adaptive flow control efforts to effectively modify the behaviors of turbulent flows.

We thank the support from the US Air Force Office of Scientific Research (FA9550-21-1-0178), Army Research Office (W911NF-19-1-0032), and Office of Naval Research (N00014-19-1-2460).

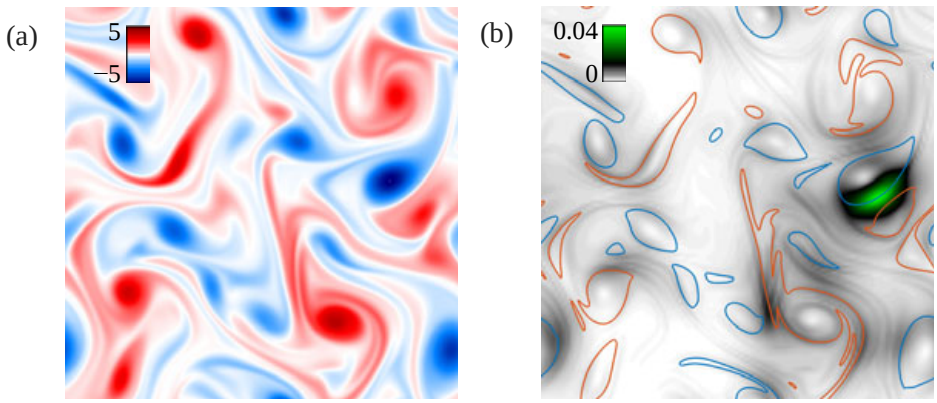

Figure 1. Network broadcast analysis of two-dimensional isotropic turbulence [5]. (a) Vorticity field. (b) Network broadcast mode. Reprinted with permission from Cambridge University Press.

References

[1] Newman, M. E. J., Networks: An Introduction. 2nd ed., Oxford Univ. Press. (2018).
[2] Taira, K. and Nair, A. G., Network-Based Analysis of Fluid Flows: Progress and Outlook, in review and available on arXiv, 1–35 (2021).
[3] Nair, A. G. and Taira, K., Network-Theoretic Approach to Sparsified Discrete Vortex Dynamics. *J. Fluid Mech.* **768**, 549–571 (2015).
[4] Taira, K., Nair, A. G., and Brunton, S. L., Network Structure of Two-Dimensional Decaying Isotropic Turbulence. *J. Fluid Mech.* **795**, R2 (2016).
[5] Yeh, C.-A., Gopalakrishnan Meena, M., and Taira, K., Network Broadcast Analysis and Control of Turbulent Flows. *J. Fluid Mech.* **910**, A15 (2021).
[6] Trefethen, L. N., Trefethen, A. E., Reddy, S. C., and Driscoll, T. A., Hydrodynamic Stability without Eigenvalues. *Science* **261**(5121), 578–584 (1993).
[7] McKeon, B. J. and Sharma, A. S., A Critical-Layer Framework for Turbulent Pipe Flow. *J. Fluid Mech.* **658**, 336–382 (2010).

ON-THE-FLY REDUCED-ORDER MODELING OF TURBULENT FLOW RESPONSE TO HIGH-DIMENSIONAL FORCING WITH TIME-DEPENDENT BASES

Hessam Babaee
Department of Mechanical Engineering, University of Pittsburgh, Pittsburgh, PA

Predicting how turbulent flow responds to high-dimensional forcing is of interest to many important problems in fluid mechanics including causality in turbulence, transition, and flow control. Clearly, finding the response of the turbulent flow to a high-dimensional forcing is computationally prohibitive as many forward samples of the direct numerical simulations of the turbulent flow are required. We present an on-the-fly reduced-order modeling technique based on forced optimally time-dependent decomposition (f-OTD) to significantly accelerate the computations. In the f-OTD formulation, the response of the system is decomposed to a set of time-dependent orthonormal bases and a set of time-dependent coefficients. We present a variational principle whose optimality conditions yield the evolution equations for the f-OTD bases and their coefficients. As a result, the f-OTD formulation does not require offline data generation to extract the f-OTD modes and because the f-OTD modes are time-dependent, they can adapt on the fly to intrinsic or externally excited flow instabilities. We will demonstrate the performance of the f-OTD formulation for several benchmark problems.

TIME-LOCALIZED RESOLVENT ANALYSIS FOR THE STUDY OF CAUSAL RELATIONS IN TURBULENT FLOWS

Eric Ballouz[1], Barbara Lopez-Doriga[3], Scott T. M. Dawson[3] and H. Jane Bae[2]
[1] *Mechanical and Civil Engineering, California Institute of Technology, Pasadena, CA 91125, USA.*
[2] *Graduate Aerospace Laboratories, California Institute of Technology, Pasadena, CA 91125, USA.*
[3] *Mechanical, Materials and Aerospace Engineering, Illinois Institute of Technology, Chicago, IL 60616, USA.*
E-mail: eballouz@caltech.edu

Resolvent analysis [2, 4] has been successfully used to study complex nonlinear phenomena, such as hairpin vortices and their associated fast pressure fluctuations in turbulent pipe flow [3], and scaling and self-similarity in turbulent channel flow [5]. In resolvent analysis, we rewrite the Navier-Stokes equation as a linear mapping between the nonlinearity, interpreted as an input, and perturbations about a steady (or periodic [6]) mean flow, the output. In this input-output formulation, the resolvent is the linear input-output map, and its operator properties shed light on the effect of nonlinearities on the mean, linearized flow. Singular value decomposition of the resolvent operator provides the orthogonal bases for the input and output spaces and helps rank the input-output mode pairs in terms of amplification by the resolvent. This framework is able to identify the dominant spatial perturbation structures in turbulent flows [3, 4, 6].

The input-output formulation has been used to investigate causality in turbulence. For turbulent channel flow, authors of [1] identify the most significant forcing mode of the resolvent at the fundamental wave number and find that removing the flow component aligned with this mode from a numerical simulation at each time step inhibits turbulence. The authors further identify the dyadic interactions of velocity that most contribute to the principal forcing mode, and reconstruct the associated flow configurations. The paper argues for a causal link between the flow configurations responsible for the dyadic interactions that produce the principal forcing mode, and the appearance of strong nonlinear forcing upon the mean flow.

However, this method does not consider temporally-local nonlinear forcing and its transient effect on the flow. Time-localization is needed to establish cause-and-effect relations, which must respect the arrow of time. We thus propose generalizing resolvent analysis to time-localized nonlinearities and flow perturbations. Given input forcing modes and the outputs they produce, one would indeed need the time localization of the input and the output to further subdivide the output into its input and output components and to draw conclusions about cause and effect in accordance with the arrow of time.

In order to obtain time-localization while retaining frequency information, the resolvent analysis can be modified to project the flow state variables onto a wavelet basis rather than a Fourier basis in time. Each wavelet acts as a band-pass filter and extracts information from a signal over a time band of a characteristic width determined by the wavelet scale, at a time position determined by the wavelet's shift.

In this work, we construct the time-localized resolvent operator for the fully developed channel flow and oscillating boundary layer flow. Given an input mode at a specific time, we bisect its associated output modes into preceding and succeeding responses with respect to the time-localized input. The temporally varying resolvent operator allows us to identify causes and effects of temporally local velocity fluctuations of different scales, in the form of nonlinear forcing.

References

[1] Bae, H. J., Lozano-Durán, A. and McKeon, B. J., Nonlinear mechanism of the self-sustaining process in the buffer and logarithmic layer of wall-bounded flows, *J. Fluid Mech.* **914**, A3 (2021).
[2] Jovanović, M. R. and Bamieh, B., Componentwise energy amplification in channel flows, *J. Fluid Mech.* **534**, 145–183 (2005).
[3] Luhar, M., A. S. Sharma, and B. J. McKeon. "On the structure and origin of pressure fluctuations in wall turbulence: predictions based on the resolvent analysis." Journal of Fluid Mechanics **751**, 38–70 (2014).
[4] McKeon, B. J. and Sharma, A. S., A critical-layer framework for turbulent pipe flow, *J. Fluid Mech.* **658**, 336–382 (2010).
[5] Moarref, Rashad, et al. "Model-based scaling of the streamwise energy density in high-Reynolds-number turbulent channels." Journal of Fluid Mechanics **734**, 275–316, (2013).
[6] Padovan, Alberto, Samuel E. Otto, and Clarence W. Rowley. "Analysis of amplification mechanisms and cross-frequency interactions in nonlinear flows via the harmonic resolvent." Journal of Fluid Mechanics **900**, A14 (2020).

UNCOVERING THE LINK BETWEEN DIMENSIONAL ANALYSIS AND CAUSALITY

Zach del Rosario[1], Lluís Jofre[2] and Gianluca Iaccarino[3]
1 *Olin College* zdr@olin.edu, 2 *Technical University of Catalonia* lluis.jofre@upc.edu, 3 *Stanford University* jops@stanford.edu

Statistical formulations of causality are designed to overcome *lurking variables* [Joi81; PB14]: important factors that are neglected by the experimenter or hidden by easily observable correlations. This focus is necessary to deal with the complexities of social and biological systems, where enormous complexity makes controlling all important factors impossible. Statistical methods are formulated to mitigate [RR83], or innoculate [BHH+78], an analysis against such lurking factors using a theory-independent approach of treatment assignment based on randomized tests. However, in the physical sciences, the ideas stemming from dimensional analysis enable a more physics-constrained approach.

The familiar Buckingham Pi theorem [Buc14] is the fundamental result of dimensional analysis, stating that any physical law involving measured quantities is necessarily a function of a smaller number of *dimensionless groups*. However, this fundamental result can be endowed with greater structure; a simple log-transform of input quantities leads to a vector subspace interpretation of dimensionless numbers [CRI16].

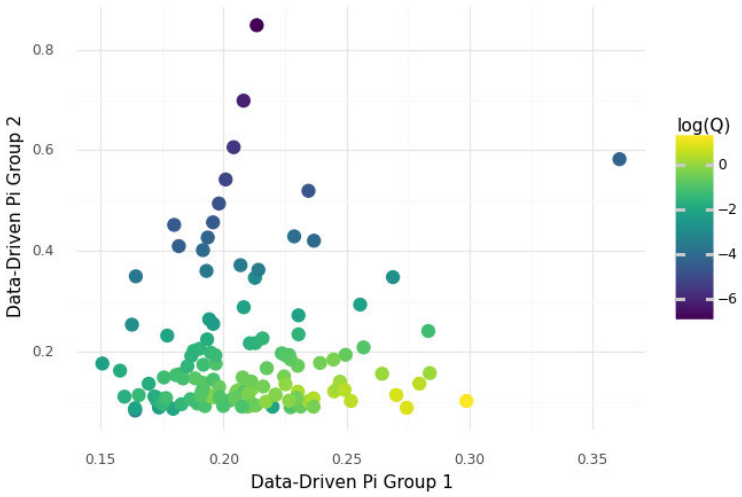

Figure 1. Data-driven dimensional analysis can identify relevant dimensionless numbers. Buckingham Pi predicts 12 dimensionless numbers for this case study; a data-driven analysis identifies two dimensionless numbers that are sufficient to describe the observed trends [JdI20].

The subspace formulation of the Buckingham Pi theorem has two important applications: (i) a formal analysis of lurking variables [RLI19]; and (ii) data-driven approaches to dimensional analysis (Fig. 1). In this talk, we review recent developments in dimensional analysis that provide a physics-constrained view of causality applied to the classical pipe flow experiments by Reynolds and a realistic dataset of particle-laden turbulent flow simulations subject to radiation.

References

[Buc14] Edgar Buckingham. "On physically similar systems; illustrations of the use of dimensional equations". In: *Phys. Rev.* 4 (4 Oct. 1914), pp. 345–376. DOI: 10.1103/PhysRev.4.345. URL: http://link.aps.org/doi/10.1103/PhysRev.4.345.

[BHH+78] George EP Box, William H Hunter, Stuart Hunter, et al. *Statistics for experimenters*. Vol. 664. John Wiley and sons New York, 1978.

[Joi81] Brian L. Joiner. "Lurking variables: Some examples". In: *The American Statistician* 35.4 (1981), pp. 227–233.

[RR83] Paul R Rosenbaum and Donald B Rubin. "The central role of the propensity score in observational studies for causal effects". In: *Biometrika* 70.1 (1983), pp. 41–55.

[PB14] Judea Pearl and Elias Bareinboim. "External validity: From do-calculus to transportability across populations". In: *Statistical Science* 29.4 (2014), pp. 579–595.

[CRI16] Paul G Constantine, Zachary del Rosario, and Gianluca Iaccarino. "Many physical laws are ridge functions". In: *arXiv preprint arXiv:1605.07974* (2016).

[RLI19] Zachary del Rosario, Minyong Lee, and Gianluca Iaccarino. "Lurking Variable Detection via Dimensional Analysis". In: *SIAM/ASA Journal on Uncertainty Quantification* 7.1 (2019), pp. 232–259. DOI: 10.1137/17M1155508. eprint: https://doi.org/10.1137/17M1155508.

[JdI20] Lluís Jofre, Zachary del Rosario, and Gianluca Iaccarino. "Data-driven dimensional analysis of heat transfer in irradiated particle-laden turbulent flow". In: *International Journal of Multiphase Flow* (Apr. 2020). DOI: 10.1016/j.ijmultiphaseflow.2019.103198.

LARGE-SCALE DYNAMICS DETERMINES THE PREDICTABILITY OF EXTREME EVENTS IN TURBULENCE

Alberto Vela-Martín, Marc Avila
ZARM, University of Bremen.
E-mail: alberto.vela.martin@zarm.uni-bremen.de

Extreme events in geophysical flows have a strong impact in human life and in diverse economical activities, and their prediction is crucial to mitigate their consequences. Particularly now, in the context of climate change, interest has emerged to develop models and indicators that allows for early detection and warning of extreme events. Some of these models have proved successful [1], but it is unclear if they can be improved because the predictability limit of extreme events is unknown: how far in advance can we predict extreme events with a perfect model? This limit is usually determined by the rate at which the uncertainty of the initial conditions is amplified by the chaotic dynamics of the system [2], i.e., by the leading Lyapunov exponent. Its inverse, the Lyapunov time, provides the time scale over which predictions become unfeasible. However, this estimate does not offer direct information on the predictability of particular features of the flow, such as the extreme bursts of a relevant quantity.

In this talk, we show that it is now possible to measure the predictability of extreme events directly by probing phase space with a computationally-intensive approach. This allows to assess the exact potential of predictive models and to determine precisely the conditions under which they may be effective. We analysed the predictability of extreme bursts of the dissipation in a two-dimensional Kolmogorov flow by producing massive ensembles of initial conditions perturbed around independent base flows. We produced millions of realisations to cover the full attractor of the Kolmogorov flow, and used the Kullback—Leibler divergence [3], an information-theoretical tool, to assess predictability. This analysis shows that extreme bursts of the dissipation may be successfully predicted beyond a few Lyapunov times, but that their predictability depends strongly on the phase-space region from which they emerge. Specifically, we reveal that predictable and unpredictable events evolve from two distinctly different large-scale circulation patterns (see figure). These results open the possibility of improving predictive models by tuning them to the large-scale dynamics. Our approach could be adapted with the available compute power to more complex flows, for instance to test the predictability of extreme relaminarisation events in transitional flows or the bursting in near-wall turbulence.

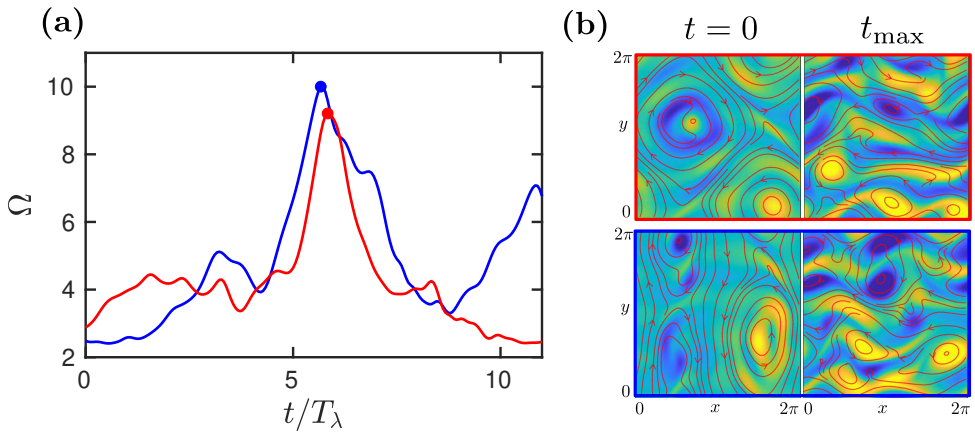

Figure 1. (a) Temporal evolution of the average entrophy, $\Omega = \langle \omega^2 \rangle$, in two independent bursts of the dissipation $\varepsilon = \nu\Omega$, where ν is the kinematic viscosity. The red line corresponds to a burst that is unpredictable at $t = 0$, while the blue line corresponds to a predictable burst. $T_\lambda = \lambda^{-1}$ and λ is the leading Lyapunov exponent. (b)Visualisation of the flow in the temporal evolution plotted in (a); red, the unpredictable burst; blue the predictable burst. Panels on the left correspond to $t = 0$, before the burst, and panels on the right to the moment of the burst, $t_{\max} = 5.5T_\lambda$ and $t_{\max} = 5.9T_\lambda$. The colors correspond to the value of the vorticity from -6 (dark blue) to 6 (ligth yellow), and the red lines to the streamlines of the velocity field.

References

[1] Farazmand, M. and Sapsis, T.P., *Science advances* **3**, e1701533 (2017).
[2] Lorenz, Edward N., *Tellus*, **17**, 321–333, (1965).
[3] DelSole, T., *J. Atmos. Sci.*, **61**, 2425–2440 (2004).

CAUSALITY IN DROP-TURBULENCE INTERACTIONS: IDENTIFYING THE DRIVER OF DROP DEFORMATION AND BREAKUP

Alberto Vela-Martín, Marc Avila
ZARM, University of Bremen.
E-mail: alberto.vela.martin@zarm.uni-bremen.de

Binary mixtures of inmiscible fluids in turbulent conditions are ubiquitous in natural phenomena and industrial applications. The physical properties of these flows depend strongly on the structure of the disperse phase, in which the breakup of fluid particles—drops or bubbles—plays a fundamental role. Understanding and modelling turbulent breakup is essential to predict and control the dynamics of inmiscible mixtures, but this remains a challenge to theoretical and empirical approaches. Fluid-particle breakup is often viewed from an energetic perspective, in which the surface energy of the particle is a marker of its degree of deformation. This approach is very convenient, but requires isolating the mechanisms that lead to the effective increments of the surface energy, and thus to breakup. Fluid-particle deformation occurs when turbulent kinetic energy is transformed into surface energy, but the opposite mechanism is also possible; fluid-particle relaxation produces turbulent kinetic energy through oscillatory motions in which the surface energy may increase locally (although not on average). Only the former mechanism can cause breakup, but distinguishing it from the latter is difficult because of the complexity of surface-turbulence interactions.

In this talk, we address this problem by resorting to causality analysis applied to drops embedded in isotropic turbulence. We leverage our recent findings on the mechanism that causes the increments of the surface energy, which may be locally described as the stretching of the drop surface by the local rate-of-strain tensor [1]. We decompose this quantity into local and non-local components, which describe the contribution to surface-energy increments due to eddies far from the drop surface (outer stretching), and close to it or inside the drop (inner stretching). We average these quantities over the surface of single drops, and construct temporal signals of the contribution to the surface energy due to inner and outer stretching that cover the evolution of drops until breakup. We study the causal relation between these signals in massive ensembles of time-resolved independent single-drop simulations at different Weber numbers (see figure 1(a)). First, we show that the temporal auto-correlation of the outer stretching scales with turbulence quantities, while that of the inner stretching scales with the characteristic relaxation time of the interface. Moreover, their cross-correlation shows that negative inner stretching (surface relaxation) occurs on average after positive outer stretching (surface deformation due to turbulence) with a time delay that scales with the relaxation time, suggesting that the latter is the cause of the former (see figure 1(b)). We corroborate this hypothesis by applying convergent cross mapping [2], a non-linear test of causality, to the signals. These results indicate that the causes of drop breakup may be largely identified by analysing the outer stretching; it depends mostly on turbulence dynamics, it is the main source of surface-energy increments, and drives the inner stretching, which acts as a rather 'passive' surface-energy dissipation mechanism.

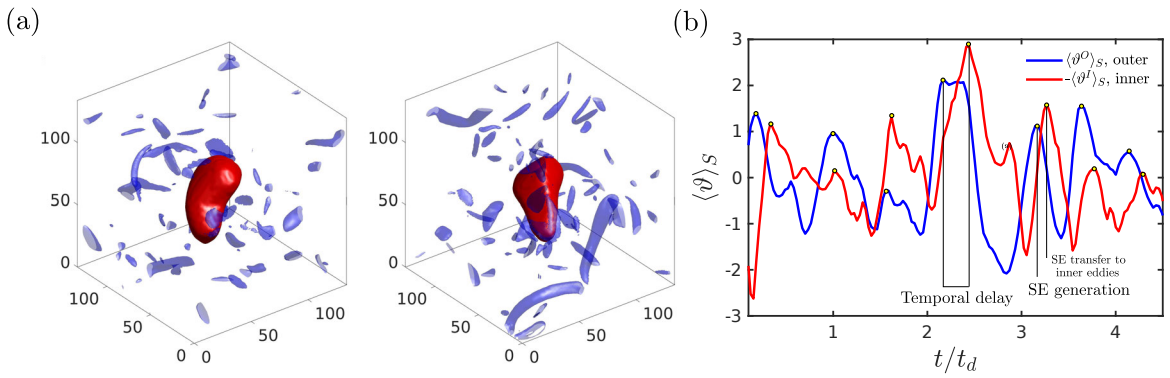

Figure 1. (a) A drop embedded in isotropic turbulence at Weber numbers $\mathrm{We} = 1.8$. The frame is fixed at the centre of the drop, blue isosurfaces mark intense vorticity. The size of the computational box is marked in Kolmogorov units. (b) Temporal evolution of the contributions to surface energy (SE) of (blue) outer and (red) inner eddies in the evolution of a single drop in isotropic turbulence.

References

[1] Vela-Martin, A, Avila, M, *J. Fluid Mech.* **929** (2021).
[2] Ye, H. and Deyle, E.R. and Gilarranz, L.J. and Sugihara, G., *Sci. Rep.* **5**, 1–9 (2015).

BUTTERFLIES IN THE ATMOSPHERE: EVALUATING LOCAL DIVERGENCE ON THE MODEL ATTRACTOR

Mark Rodwell[1]
European Centre for Medium-Range Weather Forecasts, Reading, UK.
E-mail: mark.rodwell@ecmwf.int

Global numerical weather prediction is often limited by Lorenz–type "butterflies" in the flow [1]. Here we think of these as local flow configurations associated with pronounced uncertainty growth–rates, as demonstrated in short–range ensemble predictions. Some of these configurations correspond to potential instabilities of the flow. Often, forecasts for severe downstream weather only show an improvement in skill when these butterflies have passed. Here the focus is on cyclogenesis [3] and meso-scale convective [2] butterflies in the middle latitudes. A key question is how operational ensemble forecast systems represent the uncertainty growth–rates associated with these instabilities? A "Lagrangian" growth-rate, which follows the ensemble-mean flow, is found to be a convenient approach to highlighting sources of uncertainty (Fig. 1). At short ($\sim$ 12 h) lead-times, operational forecast models differ in these growth-rates. Partly this is related to pragmatic approaches to ensemble initialisation (application of singular vector perturbations for example) and approximations for model uncertainty, but there may also be a component associated with differences in the underlying "deterministic" model. Growth-rates can be evaluated by comparing ensemble spread with ensemble-mean errors (relative to estimates of the truth — observations or analyses from data assimilation). Results suggest that growth-rates for the cyclogensis butterfly are over-estimated (indicating an un-tapped source of predictability), while for the meso-scale convective butterfly they are under-estimated (the forecast is too confident).

References

[1] E. N. Lorenz. Predictability; Does the flap of a butterfly's wings in Brazil set off a tornado in Texas? Presented at the American Association for the Advancement of Science, 139th meeting, December 1972. Archived 2013-06-12 at the Wayback Machine, Accessed: 2021-11-11.
[2] M. J. Rodwell, D. S. Richardson, D. B. Parsons, and H. Wernli. Flow-dependent reliability: A path to more skillful ensemble forecasts. *Bull. Amer. Meteor. Soc.*, 99(5):1015–1026, 2018.
[3] M. J. Rodwell and H. Wernli. The Cyclogenesis Butterfly: Uncertainty growth and forecast reliability during extratropical cyclogenesis. *Weather Clim. Dynam.*, 2022. [preprint].

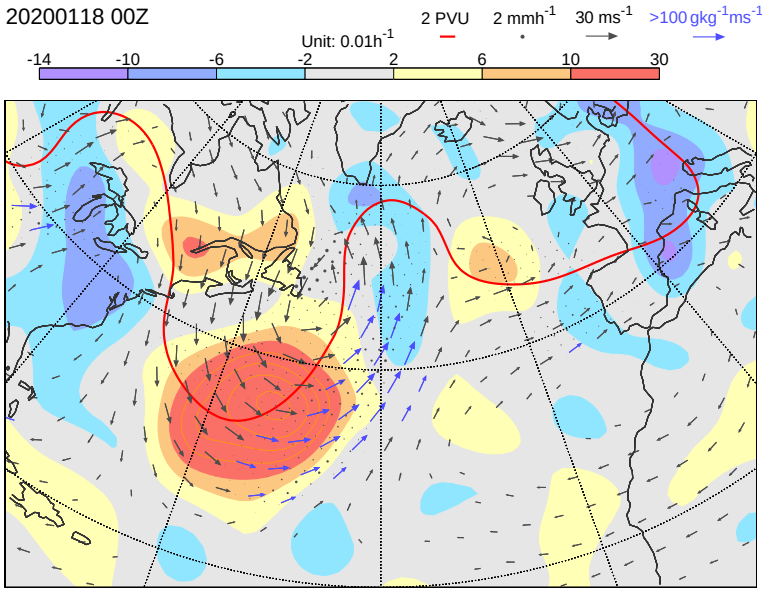

Figure 1. Single frame from an animation of cyclogenesis in the background forecasts of the ECMWF ensemble of data assimilations, focusing on synoptic spatio–temporal scales. The frame is centred at 00 UTC on 18 January 2020. The red contour shows the location of the tropopause on the 315 K isentropic upper-level surface (where potential vorticity (PV) is 2 PV Units. Vectors show horizontal winds on the 850 hPa lower-level surface (coloured blue if the moisture flux exceeds 100 $\mathrm{gkg^{-1}ms^{-1}}$). Black dots indicate ensemble–mean precipitation (the radius is proportional to the precipitation rate up to the maximum size at 2 $\mathrm{mmh^{-1}}$). Shading shoes the uncertainty growth–rate for the ensemble standard deviation of PV on 315 K (following the ensemble-mean flow). Contours extend the shading scheme to the most extreme values, which are indicated at the ends of the colour bar. Figure 3. from [3]

PREDICTABILITY OF HOMOGENEOUS ISOTROPIC TURBULENCE

Guido Boffetta[1] and Stefano Musacchio[1]
Department of Physics and INFN, University of Torino, via P. Giuria 1, 10125 Torino, Italy.
E-mail: guido.boffetta@unito.it

We discuss the chaoticity and the predictability of a turbulent flow on the basis of high-resolution direct numerical simulations at different Reynolds numbers. The maximum Lyapunov exponent of turbulence, which measures the exponential separation of two initially close solutions of the Navier-Stokes equations, is found to grow with the Reynolds number of the flow, with an anomalous scaling exponent, larger than the one obtained on dimensional grounds. For large perturbations, the error is transferred to larger, slower scales, where it grows algebraically generating an *inverse cascade* of perturbations in the inertial range. In this regime, our simulations confirm the classical predictions based on closure models of turbulence [1]. We also discuss how to link chaoticity and predictability of a turbulent flow in terms of a finite size extension of the Lyapunov exponent.

References

[1] Boffetta, G. and Musacchio S., *Phys. Rev. Lett.* **119**, 054102 (2017).

INHERENT HIGH-FREQUENCY INSTABILITIES DEVELOPING FROM SMOOTH NOISELESS INITIAL CONDITIONS

Christopher J. Sear[1], Stephen J. Cowley[1]
[1] *DAMTP, Wilberforce Road, Cambridge CB3 0WA, UK*

This talk takes a more conventional approach to causality, and considers the origin of high-frequency short-wavelength disturbances. In the case of a vortex sheet, Moore [1] showed that a finite-time curvature singularity could develop from smooth, 'noise-free', initial conditions. We demonstrate that high-frequency oscillations can develop in a finite time in solutions to the Kuramoto-Sivashinsky (KS) equation from smooth, 'noise-free', initial conditions.

This work was motivated by the calculations of Brinckman and Walker [2] who showed numerically that, because of the development of oscillations with asymptotically short wavelengths, unsteady high-Reynolds-number solutions of the Navier-Stokes (NS) equations do not always converge to unsteady *regular* solutions of the boundary-layer equations. Cowley [3] argued heuristically that these oscillations were Rayleigh instabilities triggered by one or more singularities in complex space.

We believe that our analysis sheds light on the origin of short-wavelength disturbances in high-Reynolds-number flows. We restrict attention to the KS equation because the analysis of the complex-space structure of solutions to the NS equations is difficult in two or three spatial dimensions. The KS equation shares the key properties of the NS equation that are responsible for the instability, i.e. the KS equation possesses a destabilising term for a range of high wavenumbers, and it is non-linear, allowing these destabilising modes to be filled out in the Fourier spectrum (even if no such modes are present in the initial condition). Further, the kinematic-wave equation, as an asymptotic limit of the KS equation, is analogous to the role of the boundary-layer equation as an asymptotic limit of the NS equation. Hence, as well as illustrating the genesis of high-frequency instabilities, we believe that our analysis indicates why unsteady solutions of the NS equations do not always converge to solutions of the boundary-layer equations at high Reynolds numbers. More specifically, by considering exponentially small terms in an unsteady asymptotic solution of the KS equation in the complex plane (and in particular by considering various Stokes and anti-Stokes lines), we can predict the asymptotic breakdown of *regular* kinematic-wave solutions by short-wave instabilities. These instabilities can develop at far smaller times than the formation of, say, shocks in kinematic-wave solutions; naïvely, one might have expected that the shock-formation time would have been when short-wavelength disturbances would have developed.

References

[1] D.W. Moore, The spontaneous appearance of a singularity in the shape of an evolving vortex sheet. *Proc. R. Soc. Lond. A*, **365**, 105-119, 1979.
[2] K.W. Brinckman and J.D.A. Walker, Instability in a viscous flow driven by streamwise vortices. *J. Fluid Mech.*, **432**, 127-166, 2001.
[3] S.J. Cowley, Laminar Boundary-layer Theory: A 20th Century Paradox? In: Aref H., Phillips J.W. (eds) Mechanics for a New Millennium. Springer, Dordrecht, 2002.

CAUSE AND EFFECT IN TURBULENCE - A STATISTICAL POINT OF VIEW

Martin Oberlack[1,*] and Sergio Hoyas[2]
[1]*Technical University Darmstadt, Chair of Fluid Dynamics, Otto-Bernd-Str. 2, 64287 Darmstadt, Germany*
[*]*E-mail: oberlack@fdy.tu-darmstadt.de*
[2]*Instituto Universitario de Matemática Pura y Aplicada, UP València, Camino de Vera, 46024 València, Spain*

Classical questions of *cause* and *effect* concern the temporal invertibility and are already a very fundamental problem for spatio-temporally parabolic equations such as the Navier-Stokes equations, e.g. when considering linear or weakly nonlinear stability problems. If the system then shows strongly chaotic properties, questions of invertibility for large time horizons are hardly treatable.

One way out of this dilemma is a statistical view of turbulence, and indeed the turbulence community considers a variety of statistical laws such as Kolmogorov's scaling laws to be absolutely fundamental. This complicates matters further, however, because then cause and effect are no longer as clear-cut as Navier-Stokes would have us believe even on small time horizons.

In the statistics of Navier-Stokes processes, the time direction is of course not changed, but formally instantaneous processes "run in parallel", or, in the case of statistically stationary processes, time levels are thus even "interwoven" with each other.

This complicates its treatment considerably, because cause and effect now take on a different meaning. To illustrate this, let us consider heat conduction through the molecular motion in gases as an example system, even if the analogy to Navier-Stokes is not ideal. On the level of molecular interaction processes, the underlying dynamic system is still reversible. On a statistical level, however, this is no longer true because, as is well known, entropy increases and this is accompanied by the "birth" of two symmetries in the heat conduction equation that do not exist in the original dynamic system for the molecules. These symmetries prevent the reversal of the arrow of time and, at the same time, one of the symmetries generates the fundamental solution of the heat conduction equation. The heat equation is formally parabolic in space-time and thus principally non-invertible.

In the statistics of turbulence, something rather similar happens, because the infinite-dimensional statistical systems such as the Hopf functional equation or the Lungren hierarchy admit further so-called statistical symmetries that go beyond those of the Navier-Stokes equations and characterise intermittency and non-Gaussian behaviour [3, 4]. In the recent coupled PRL/PRF publications [2, 1], we have been able to show that it is especially these statistical symmetries that determine the statistics of the process in turbulent shear flows, i.e. are central for the correct description of high velocity moments . Therein, invariant solutions for the statistics of high moments have been generated (the corresponding invariant PDF solutions also exist; a publication on this is in preparation and results will be shown at the conference). It should be noted that these are fundamentally different from the "invariant solutions" that are currently being intensively discussed in structure formation processes in transitional and low-Re turbulent flows. In this field, only classical Navier-Stokes symmetries are used, such as (spatial) reflections and the like.

However, there is a fundamental difference between the symmetries admitted by the heat conduction equation and those in turbulence, namely that the statistical symmetries of turbulence are formally infinite-dimensional. This formally implies a freedom in the "choice of symmetries", and we do not know how turbulence "chooses" them in a concrete case.

Here we come full circle to the question of cause and effect in turbulence and this goes beyond the question of whether there is a spatio-temporal connection between cause and effect. Two central questions will be addressed: (i) We do see very clearly the effect in the choice of the statistical symmetries "picked by turbulence" and the corresponding solutions for the moments. However, the concrete choice of symmetries, i.e. the cause, remains unclear; (ii) The question where the statistical symmetries come from, i.e. what is the cause of its appearance goes even deeper, because the presence of the symmetries, i.e. the effect, is very clearly visible e.g. in [2] .

Regarding question (i), we already have a clear proposal, namely that the cause and effect of the turbulence statistics are connected by an eigenvalue problem of the Lundgren hierarchy based on the statistical symmetries, which will be presented in its first outlines at the conference. Question (ii) goes even deeper. Here, finally, the comparison with heat conduction should be made again. The key principle underlying the heat conduction process is the entropy inequality, but something analogous is not yet known for turbulence - a largely unresolved question.

References

[1] S. Hoyas et al. Wall turbulence at high friction reynolds numbers. *Phys. Rev. Fluids*, 7:014602, 2022.
[2] M. Oberlack et al. Turbulence statistics of arbitrary moments of wall-bounded shear flows: A symmetry approach. *Phys. Rev. Lett.*, 128:024502, 2022.
[3] M. Oberlack and A. Rosteck. New statistical symmetries of the multi-point equations and its importance for turbulent scaling laws. *Discrete & Continuous Dynamical Systems - S*, 3(3):451–471, 2010.
[4] M. Wacławczyk et al. Statistical symmetries of the lundgren-monin-novikov hierarchy. *Phys. Rev. E*, 90:013022, 2014.

VARIABILITY OF THE FLOW AROUND AN IMPULSIVELY STARTED PITCHING BLADE

Jerry Westerweel, Ernst Jan Grift and Mark Tummers
Laboratory for Aero & Hydrodynamics, TU Delft, The Netherlands.
E-mail: j.westerweel@tudelft.nl

The motion of fluid flow is described by the continuity equation and the Navier-Stokes equations, where the development of the flow is determined by the initial and boundary conditions. The Navier-Stokes equations are non-linear, so that the actual flow development depends sensitively on the initial conditions. Since the initial conditions can only be determined with finite precision, any two solutions of the equations of motion with initial conditions that differ only by a very small amount, will eventually diverge, as the small initial differences propagate and grow exponentially with time; this is commonly referred as the 'Butterfly effect', coined after the shape of the Lorenz attractor and the dynamical behaviour of the non-linear dynamical system it represents [3, 4].

We employ particle image velocimetry (PIV) to study the motion induced by an accelerating and pitching cambered plate using an industrial robot to precisely control the motion [1, 2]. The Reynolds number is 2.2×10^5. Initially a boundary layer forms and leading edge and trailing vortices are formed, after which the flow quickly transitions to a disordered turbulent flow state. When repeating such measurements, one would expect that the turbulent flow in individual repetitions would quickly become uncorrelated, in particular for the small-scale turbulent flow structure. However, contrary to this expectation, the small-scale structure of the flow remains highly correlated, as is illustrated in Figure 1 by measurements in three *separate* runs; please note the high degree of similarity of the detailed vortical flow structures, despite the high Reynolds number.

To characterise how causality in the generation of a flow can be characterised in such experiments, we consider the Lagrangian trajectories of virtual particles in the measured flow field, and consider the separation $||\delta\mathbf{x}||$ between individual realisations. We compute the local finite-time Lyapunov exponents [5]. Despite the turbulent nature of the flow, the overall growth of $||\delta\mathbf{x}||$ appears to be linear, i.e. $||\delta\mathbf{x}|| = ct$, with $c = 0.004$ [m/s]; this implies a separation of 4 [mm] at the end of the motion, which is still less than the resolution of the measurement (6 [mm]). A smaller section of the flow displays exponential growth of $||\delta\mathbf{x}|| \sim \exp(\sigma t)$, with: $\sigma \cong 5$ [s^{-1}]; this corresponds to only 10 [mm] for the results presented in Fig. 1. The question remains when such a flow transits from a chaotic to a truly turbulent flow state.

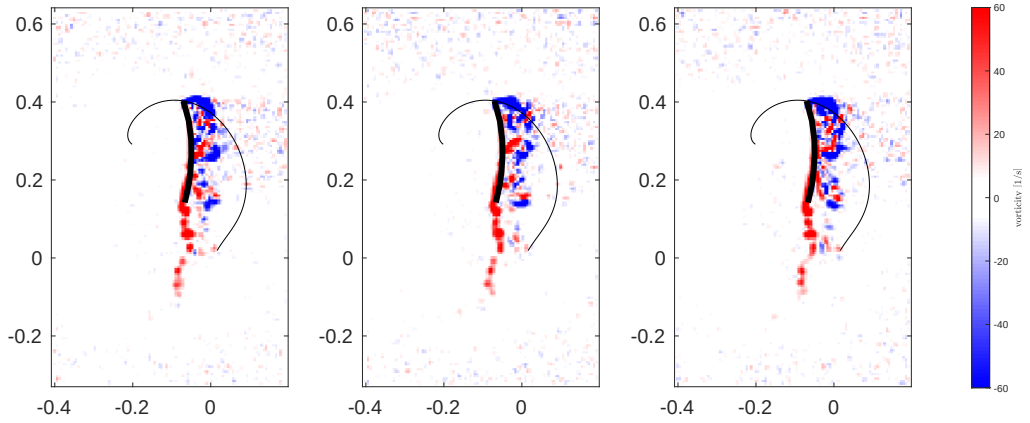

Figure 1. Three individual realisations of the motion of a translating and pitching cambered plate blade at time $t = 0.528$ s after the start of the motion, depicting the out-of-plane component of the vorticity computed from planar PIV data. Note the detailed resemblance of the small-scale vortical structures. The Reynolds number is 2.2×10^5. (Dimensions are in [m].)

References

[1] Grift, E.J., Tummers, M.J., Westerweel, J.: Hydrodynamics of rowing propulsion. J. Fluid Mech. **918**, A29 (2021)
[2] Grift, E.J., Vijayaragavan, N.B., Tummers, M.J., Westerweel, J.: Drag force on an accelerating submerged plate. J. Fluid Mech. **866**, 369–398 (2019)
[3] Lorenz, E.N.: Deterministic nonperiodic flow. J. Atmos. Sci. **20**, 130–141 (1963)
[4] Schuster, H.G.: Deterministic Chaos. Physik-Verlag, Weinheim, D (1984)
[5] Shadden, S.C., Lekien, F., Marsden, J.E.: Definition and properties of Lagrangian coherent structures from finite-time Lyapunov exponents in two-dimensional aperiodic flows. Physica D **212**, 271–304 (2005)

GENERALISED QUASILINEAR APPROXIMATIONS OF TURBULENT CHANNEL FLOW. STREAMWISE NONLINEAR ENERGY TRANSFER

Carlos González Hernández[1], Qiang Yang[2] and & Yongyun Hwang[1]
[1]*Department of Aeronautics, Imperial College London*
[2]*State Key Laboratory of Aerodynamics, China Aerodynamics Research and Development Centre*
E-mail: cg1116@ic.ac.uk

A generalised quasilinear (GQL) approximation [1, 2] is studied in turbulent channel flow at $Re_\tau \simeq 1700$ (Re_τ is the friction Reynolds number). The focus of the present study is given to its application in the streamwise direction to explore the nonlinear interactions between energy-containing streamwise waves, which have been understood to originate from the streak instability and/or transient growth mechanism in the self-sustaining processes at different length scales. Waves, vortices and streaks are interrelated (causal) in wall-bounded turbulent shear flows; e.g. there cannot be streaks without vortices and viceversa. In this fashion, the GQL approximation provides a robust interventional tool to explore scale interactions, given that it is capable of suppressing particular triadic interactions in a controlled manner [3]. The GQL approximation decomposes the flow into two groups, the former of which contains a set of low-wavenumber Fourier modes and the latter are composed of the rest high-wavenumber modes. The former low-wavenumber group is then solved by considering the full nonlinear equations, while the latter high-wavenumber group is obtained from the linearised equations around the former. The performance of the GQL approximation is compared with that of the QL model [4], in which the low-wavenumber group only contains zero streamwise wavenumber. The QL case has been found to exhibit the most anisotropic second-order turbulence statistics throughout the entire wavenumber space of the spectra, in agreement with the previous studies [4, 5]. Only a small increase in the number of streamwise modes allowed to interact nonlinearly has resulted in a rapid recovery of the scaling of the streamwise wavelengths with the distance from the wall, which was absent in the streamwise spectra of the QL case. These cases also exhibited spectra extending over a wider range and reaching out to smaller scales, when compared to the QL case whose spatial spectra were highly localised in the wavenumber space. The production spectra of the QL model have also been found to be highly localized and the turbulent transport is inhibited in the streamwise direction. In effect, it is found that the QL model exhibits a considerably reduced multi-scale behaviour at the given moderately high Reynolds number. Finally, it is proposed that the energy transfer from the low to the high-wavenumber group in the GQL approximation, referred to as the 'scattering' mechanism [2], depends on the neutrally stable leading Lyapunov spectrum of the linearised equations for the high wavenumber group. This has explained the gradual extension of the spectra of the GQL model over a wider range, when the cut-off streamwise wavelength for the velocity decomposition in the GQL model is sufficiently large. This is also consistent with the emergence of the trivial solution in the high-wavenumber group, when the cut-off wavelength is sufficiently small (figure 1).

C. G. H. and Y. H. acknowledge the support of the Leverhulme trust (RPG-123-2019).

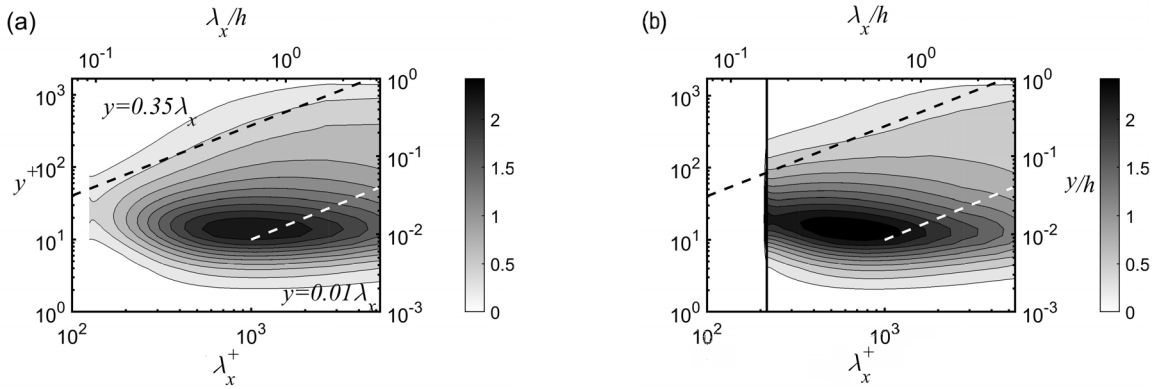

Figure 1. Premultiplied streamwise wavenumber spectra of $k_x^+\Phi_{uu}^+(y^+, \lambda_x^+)$ for (a) LES and (b) GQL25 (25 streamwise modes).

References

[1] Marston, J. B., Chini, G. P. and Tobias, S. M., Generalized quasilinear approximation:Application to zonal jets. *Phys. Rev. Lett.* **116**, 214501 (2016)

[2] Tobias, S. M. and Marston, J. B., Three-dimensional rotating Couette flow via the generalised quasilinear approximation. *J. Fluid Mech.* **810**, 412–428 (2017)

[3] Hernández, C. G., Yang, Q. and Hwang, Y., Generalised quasilinear approximations of turbulent channel flow: Part 2. Spanwise scale interactions. *J. Fluid Mech.* **arXiv** (2021)

[4] Thomas, V. L., Lieu, B. K., Jovanović, M. R., Farrell, B. F., Ioannou, P. J. and Gayme, D. F., Self-sustaining turbulence in a restricted nonlinear model of plane Couette flow. *Phys. Fluids* **26**(10), 105112 (2014)

[5] Farrell, B.F., Ioannou, P.J., Jiménez, J., Constantinou, N.C., Lozano-Durán, A. and Nikolaidis, M-A, A statistical state dynamics-based study of the structure and mechanism of large-scale motions in plane Poiseuille flow. *J. Fluid Mech.* **809**, 290–315 (2016)

INVARIANT SOLUTIONS AND CAUSALITY IN TURBULENCE

Genta Kawahara
Graduate School of Engineering Science, 1-3 Machikaneyama, Toyonaka, Osaka 560-8531, Japan
E-mail: kawahara@me.es.osaka-u.ac.jp

It has been well known that the self-sustaining process [1] in the minimal flow unit [2] is interpreted theoretically as nonlinear equilibrium represented by simple invariant solutions, such as a fixed point [3] and a periodic orbit [4], to the Navier–Stokes equation. We believe that this theoretical interpretation can be extrapolated to self-sustaining structure and dynamics in the buffer layer of near-wall turbulence, in which the sustaining turbulence exhibits essentially a single scale in space and time. However, spatially or temporally multiscale realisations have been observed in wall turbulence [5]. The former are large-scale structures irrupting into the near-wall region, while one example of the latter is intermittent bursting associated with vigorous turbulence activity. Such spatially or temporally multiscale structures and events in turbulence are beyond the characterisation by simple invariant solutions of a single scale in space and time.

In this talk, causation of spatially or temporally multiscale realisations in turbulence is discussed in terms of the known invariant solutions to the Navier–Stokes equation and their connecting orbits in phase space. Large-scale turbulent oblique stripes have been observed commonly in transitional plane Couette and Poiseuille flows [6]. They consist of a number of smaller-scale low-velocity streaks and associated streamwise vortices, i.e. the minimal flow units. Similar large-scale oblique stripes have also been found even in fully developed turbulent boundary layers and channels at high Reynolds numbers [7]. Recently, Reetz, Kreilos and Schneider [8] have found a multiscale steady solution to the Navier–Stokes equation that resembles oblique stripe patterns in plane Couette flow. The multiscale equilibrium arises from the spatially doubly subharmonic instability of the Nagata steady solution [3]. The bifurcated invariant solution explains the origin of the large-scale oblique turbulence structure in transitional wall-bounded shear flow. As in wall turbulence, hierarchical turbulence structures have been observed in Rayleigh–Bénard convection, i.e. wall-bounded thermal convection [9]. The recently found three-dimensional steady solution [10] to the Boussinesq equation for Rayleigh–Bénard convection reveals the widely observed scaling law of heat transfer, $Nu \sim Ra^{1/3}$ (Nu and Ra being the Nusselt number and the Rayleigh number, respectively), as well as the multiscale structure consisting of larger-scale thermal convection and near-wall plumes which become smaller at higher Rayleigh numbers, suggesting that the causality of the hierarchical structure in convective turbulence could be traced to multiscale nonlinear equilibrium achieving a high heat flux.

Homoclinic and heteroclinic orbits to the periodic edge states [4] have been found in minimal plane Couette turbulence at low Reynolds numbers [11, 12]. Bursting events in the minimal flow unit can be characterised in terms of occasional excursions from the invariant solution embedded in turbulence along its homoclinic orbit. However, bursting in fully developed wall turbulence at higher Reynolds numbers cannot be interpreted as a connecting orbit to such a simple invariant solution. Recently, another turbulent attractor has been identified in a relatively small periodic box for plane Couette flow at high Reynolds numbers, exhibiting wavy large-scale streaks with vigorous turbulence activity in comparison to commonly observed Couette turbulence [13]. In a larger periodic box, this attractor would be a turbulent saddle unstable to spatially subharmonic perturbations, and transient approach to the wavy vigorous saddle along its connecting orbit in phase (sub)space might be the causation of multiscale bursting events in plane Couette turbulence at high Reynolds numbers.

References

[1] Waleffe, F. On a self-sustaining process in shear flows, *Phys. Fluids* **9**-4, 883–900 (1997).
[2] Jiménez, J. and Moin, P. The minimal flow unit in near-wall turbulence, *J. Fluid Mech.* **225**, 213–240 (1991).
[3] Nagata, M. Three-dimensional finite-amplitude solutions in plane Couette flow: bifurcation from infinity, *J. Fluid Mech.* **217**, 519–527 (1990).
[4] Kawahara, G. and Kida, S. Periodic motion embedded in plane Couette turbulence: regeneration cycle and burst, *J. Fluid Mech.* **449**, 291–300 (2001).
[5] Jiménez, J. Coherent structures in wall-bounded turbulence, *J. Fluid Mech.* **842**, P1 (2018).
[6] Tuckerman, L. Chantry, M. and Barkley, D. Patterns in wall-bounded shear flows, *Annu. Rev. Fluid Mech.* **52**, 343–367 (2020).
[7] Sillero, J. A., Jiménez, J. and Moser, R. D. Two-point statistics for turbulent boundary layers and channels at Reynolds numbers up to $\delta^+ \approx 2000$, *Phys. Fluids* **26**, 105109 (2014).
[8] Reetz, F., Kreilos, T. and Schneider, T. M. Exact invariant solution reveals the origin of self-organized oblique turbulent-laminar stripes, *Nat. Commun.* **10**, 2277 (2019).
[9] Berghout, P., Baars, W. J. and Krug, D. The large-scale footprint in small-scale Rayleigh–Bénard turbulence, *J. Fluid Mech.* **911**, A62 (2021).
[10] Motoki, S., Kawahara, G. and Shimizu, M. Multi-scale steady solution for Rayleigh–Bénard convection, *J. Fluid Mech.* **914**, A14 (2021).
[11] van Veen, L. and Kawahara, G. Homoclinic tangle on the edge of shear turbulence, *Phys. Rev. Lett.* **107**,114501 (2011).
[12] Lustro, J. R. T., Kawahara, G., van Veen, L., Shimizu, M. and Kokubu, H. The onset of transient turbulence in minimal plane Couette flow, *J. Fluid Mech.* **862**, R2 (2019).
[13] Watanabe, D., Kawahara, G. and Shimizu, M. Unprecedented turbulence in plane Couette flow, in preparation (2022).

ULTIMATE HEAT TRANSFER IN COHERENT THERMAL CONVECTION

Shingo Motoki[1], Genta Kawahara[1] and Masaki Shimizu[1]
[1]*Graduate School of Engineering Science, Osaka University, 1-3 Machikaneyama, Toyonaka, Osaka 560-8531, Japan*
E-mail: motoki.shingo.es@osaka-u.ac.jp

Rayleigh–Bénard convection is one of the most canonical flows and the fundamental problem in hydrodynamic stability theory. When the Rayleigh number Ra (dimensionless temperature difference) reaches a certain critical value, convection occurs and becomes turbulent eventually as Ra increases. One of the primary interests in convective turbulence is the scaling law of the Nusselt number Nu (dimensionless vertical heat flux) with Ra, and two power laws for very high Ra, the 'classical' scaling $Nu \sim Ra^{1/3}$ and the 'ultimate' scaling $Nu \sim Pr^{1/2}Ra^{1/2}$ (where Pr is the Prandtl number), have been intensively discussed (see e.g. Ref. [1]). The classical scaling has been reported in many experiments and numerical simulations, and recently found for nonlinear steady solutions to the Oberbeck–Boussinesq equations [2, 3, 4]. On the other hand, the ultimate scaling has not been observed yet in conventional Rayleigh–Bénard convection.

Recently, it has been numerically found that the ultimate scaling can be achieved in thermal convection between permeable walls [5]. In the simulation, the vertical transpiration velocity on the walls is assumed to be proportional to the local pressure fluctuation (Jiménez *et al.*, 2001 [6]). In the present work, we have employed the permeable-wall condition and obtained steady solutions for thermal convection between horizontal, no-slip and permeable walls with a distance H and a constant temperature difference ΔT by using the Newton–Krylov iteration (for details, see Ref. [7]).

Figure 1(*a*) shows Nu of the two-dimensional (2-D) and three-dimensional (3-D) steady solutions and the turbulent state in the thermal convection between permeable walls as a function of Ra. The ultimate scaling $Nu \sim Ra^{1/2}$ can be observed at high Ra in both steady and turbulent states. It is also confirmed that the steady solutions exhibit higher heat transfer than those in the turbulent state. Thermal and flow structures of the 2-D and 3-D steady solutions at $Ra = 10^7$ are shown in figures 1(*b,c*). In the steady ultimate states, the buoyancy induces remarkable large-scale thermal plumes fully extending from one wall to the other, leading to strong vertical velocity of the order of the terminal velocity U as well as intense temperature fluctuation of $O(\Delta T)$. Consequently, the wall-to-wall heat flux scales with $U\Delta T$ independent of thermal diffusivity, although the heat transfer on the walls is dominated by thermal conduction.

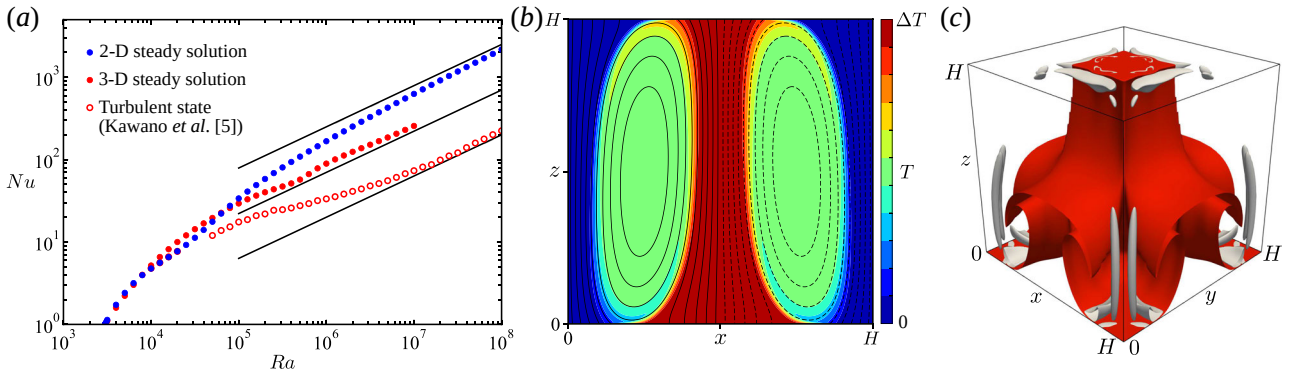

Figure 1. Steady and turbulent thermal convection between permeable walls with the permeability parameter $\beta U = 3$ for the horizontal period $L/H = 1$ and $Pr = 1$. (*a*) Nu as a function of Ra. The black lines indicate the ultimate scaling $Nu \sim Ra^{1/2}$. (*b*) Temperature and flow fields of the 2-D steady solution at $Ra = 10^7$. Large-scale counter-clockwise (or clockwise) rolls are visualised by the black solid (or dashed) streamlines. (*c*) Thermal and vortical structures of the 3-D steady solution at $Ra = 10^7$. The red and grey objects, respectively, represent the isosurfaces of the high temperature and of the positive second invariant of the velocity gradient tensor.

References

[1] Ahlers, G., Grossmann, S. and Lohse, D., *Rev. Mod. Phys.* **81**, 503–537 (2009).
[2] Sondak, D., Smith L. M. and Waleffe F., *J. Fluid Mech.* **784**, 565–595 (2015).
[3] Wen, B., Goluskin, D. and Doering, C. R., *J. Fluid Mech.* **933**, R4 (2022).
[4] Motoki, S., Kawahara, G. and Shimizu, M., *J. Fluid Mech.* **914**, A14 (2021).
[5] Kawano, K., Motoki, S., Shimizu, M. and Kawahara, G., *J. Fluid Mech.* **914**, A13 (2021).
[6] Jiménez, J., Uhlmann, M., Pinelli, A. and Kawahara, G., *J. Fluid Mech.* **442**, 89–117 (2001).
[7] Motoki, S., Kawahara, G. and Shimizu, M., *Philos. Trans. R. Soc.* in press (2022).

NEW CLASS OF SOLUTIONS IN PLANE COUETTE FLOW

Masato Nagata
Graduate School of Engineering, Department of Aeronautical and Astronautical Engineering,
Kyoto University, Nishikyo-ku, Katsura, Kyoto 615-8246 Japan
E-mail: nagata.masato.45x@st.kyoto-u.ac.jp

A new class of nonlinear solutions in the plane Couette flow (PCF) system is discovered. The solutions are obtained by a homotopy continuation from the axisymmetric Taylor vortex flow in the limit of narrow gap between coaxial cylinders which are rotating independently.

The Taylor-Couette system is controlled by the two Reynolds numbers, R_o and R_i, defined by $R_o = \frac{\omega_o r_o d}{\nu}$ and $R_i = \frac{\omega_i r_i d}{\nu}$, based on the radii, r_o and r_i, of the outer and inner cylinders which are rotating with the angular velocities, ω_o and ω_i, respectively, where ν is the kinematic viscosity and $d = r_o - r_i$ is the gap. The present analysis starts with a derivation of the correct form of equations of motion for the Taylor-Couette system in the narrow gap limit, which are parameterized by the Reynolds number, $\mathscr{R} = \frac{\omega_i(1-\mu)\overline{r}d}{\nu}$, and the rotation number, $\Omega = \frac{\omega_i(1+\mu)d^2}{\nu}$, where $\overline{r} = \frac{r_o+r_i}{2}$ is the average radius and $\mu = \frac{\omega_o}{\omega_i}$ is the angular velocity ratio. From these definitions of $\mathscr{R}$ and Ω, we find that

$$\Omega = 2\mathscr{R}\frac{1-\eta}{1+\eta}\frac{1+\mu}{1-\mu}, \qquad (\mu \neq 1), \tag{1}$$

where $\eta = \frac{r_i}{r_o}$ is the radius ratio, so that $\Omega \to 0$ as $\eta \to 1$ for a fixed value of $\mathscr{R}$, namely, the system is reduced to the PCF system in the narrow gap limit. However, this limit must be considered in such a way that the product of Ω and $\mathscr{R}$ remains finite, as the system is known to become unstable to infinitesimal axisymmetric perturbations at a finite value of the Taylor number, $T_a = \Omega(\mathscr{R} - \Omega)$ (see, for instance, [1]). Recall that the PCF system ($\Omega = 0$) never becomes linearly unstable for any $\mathscr{R}$. (Note the narrow gap limit corresponds to the Rayleigh line $\Omega = \mathscr{R}$ for μ=1 as examined in [2].)

After linear instabilities for various μ by the past stability analyses [1] are confirmed, resulting nonlinear states of axisymmetric Taylor vortex flow (TVF) bifurcating from circular Couette flow are obtained. It is found that axisymmetric TVF possesses both anti-symmetric and symmetric mean flow components (see $\check{U}_{anti}(z)$ and $\check{U}_{sym}(z)$ in Figure 1(a)). Then, by exploiting the property that axisymmetric flows depend only on T_a, irrespectively on the values of Ω and $\mathscr{R}$ provided $\Omega(\mathscr{R}-\Omega)$ remains the same, attempts are made to search for a homotopy continuation route of three-dimensional wavy vortex flows (WVF) from the axisymmetric TVF branch at finite $\mathscr{R}$, by using Ω as a homotopy parameter (see Figure 1(b)). The figure shows the existence of new PCF solutions indicated by open circles at $\Omega = 0$ along the continuation routes before reaching the PCF solutions of [3] indicated by black squares. It is found that the new solutions inherit the property of the axisymmetric TVF in the narrow gap limit, namely the symmetric mean flow component. Recall that those solutions known to exist so far in PCF, such as [3, 4], are all characterized by the mean flows which are anti-symmetric.

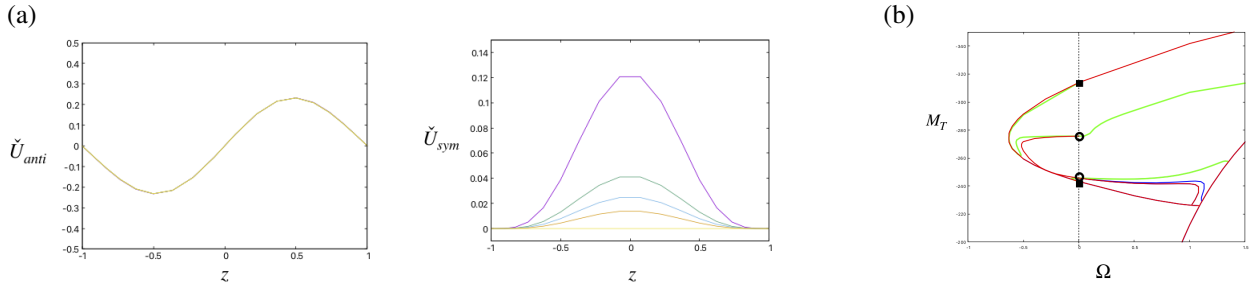

Figure 1. (a) Anti-symmetric (left) and symmetric (right) mean flow components of axisymmetric TVF where $z = \frac{r-\overline{r}}{d/2}$. μ =1.0, 0.5, 0.25, 0.0, -0.5 from bottom to top. $T_a = 150$. (b) Bifurcation of WVF with respect to the momentum transport, M_T. $\mathscr{R} = 150$. red: μ=1.0, blue: μ=0.9, green: $\mu = 0.5$. Black squares: the PCF solutions in [3]. Open circles: new PCF solutions.

Further investigations of the flow fields of the new solutions would contribute toward the study of turbulent transport in conjunction with the similarity between the narrow-gap Taylor-Couette system and Rayleigh-Bénard convection [5].

References

[1] Drazin, P. G. and Reid, W. H. *Hydrodynamic stability.* Cambridge University Press (1981)
[2] Nagata, M. Bifurcations in Couette flow between almost corotating cylinders. *J. Fluid Mech.* **169**, 229-250 (1986).
[3] Nagata, M. Three-dimensional finite-amplitude solutions in plane Couette flow: bifurcation from infinity. *J. Fluid Mech.* **217**, 519–527 (1990).
[4] Kawahara, G. and Kida, S. Periodic motion embedded in plane Couette turbulence: regeneration cycle and burst. *J. Fluid Mech.* **449**, 291-300 (2001).
[5] Busse, F. H. The twins of turbulence research. *Physics* **5**, 4 (2012).

CAUSALITY IN SEDIMENTARY TURBULENT CHANNEL FLOWS

Markus Scherer and Markus Uhlmann
Institute for Hydromechanics, Karlsruhe Institute of Technology (KIT), Karlsruhe, Germany.
E-mail: markus.scherer@kit.edu

Recently, direct numerical simulations have provided evidence that the information exchange between the near–wall and the outer region of turbulent channel flows is an asymmetric process, with information being preferentially transported from the outer flow towards the wall [2]. Causalitywise, this observation implies that the flow structures in the outer layer exert a significant influence on the dynamics of their counterparts in the near–wall region [4], whilst the impact of the latter on the outer layer structures seems to be limited. Compared to the canonical case, the causal relations between outer and near–wall dynamics in hydraulic free–surface flows over mobile sediment beds are less well understood. In this talk, we discuss as an example for an open causality problem in hydraulics the development of streamwise–aligned sediment ridges on an initially flat mobile sediment bed sheared by a turbulent open channel flow (cf. figure 1). While these sediment ridges are well–known to closely interact with secondary currents of Prandtl's second kind, it remains unclear whether a lateral bed variation causes the formation of secondary flow patterns in a 'bottom–up mechanism' or whether, *vice versa*, a spanwise variation of the turbulent flow is responsible for the evolution of the characteristic bedforms implying a 'top–down mechanism' [5].

By means of interface–resolved direct numerical simulations incorporating an immersed boundary technique and a discrete element model [7, 3], we show that the formation of sediment ridges is controlled by the outer large–scale velocity streaks and associated Reynolds stress–carrying structures in a 'top–down mechanism' that is in line with the concept of causality in canonical single–phase channel flows outlined in [2]. In this context, two–point two–time correlations reveal that the sediment bed evolution follows the dynamics of the large–scale structures in the channel bulk with a delay of several bulk time units, underlining the causal relation between both. The large–scale flow structures induce spanwise–alternating regions of low and high bed shear stress and thus lead to a locally reduced or enhanced erosion activity. The eroded sediment concentrates in a rather thin but intense sediment transport layer above the bed that disrupts the classical buffer–layer processes. The dynamics of the largest–scale structures in the channel bulk, on the other hand, do not significantly differ from those in single–phase smooth–wall open channels, thereby supporting earlier observations over fully–rough bottom walls according to which the outer flow is essentially unaffected by the details of the near–wall dynamics [6, 1].

Funding The current work was supported by the German Research Foundation (DFG) through grant UH242/12-1.

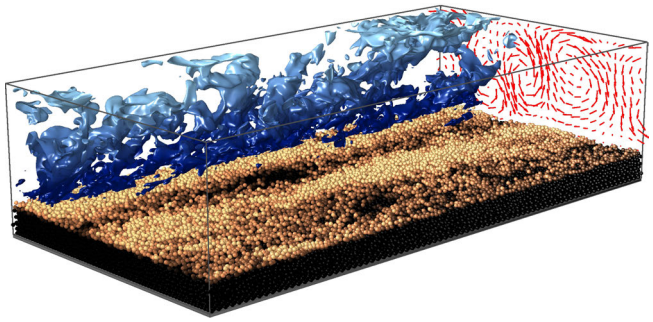

Figure 1. Instantaneous snapshot of sediment ridges and troughs together with a large–scale low–speed streak, visualised as isosorface of the streamwise velocity fluctuation u'. Brighter particle colours indicate a larger distance to the bottom wall. The mean secondary flow pattern is shown as vector plot at the downstream end of the periodic domain, main flow is from bottom left to top right. Simulation parameters: $Re_b = 9500$, $Re_\tau = 830$, $Ga = 57$, $\rho_p/\rho_f = 2.5$, $H_f/D = 25$.

References

[1] O. Flores, J. Jiménez, and J. C. Del Álamo. Vorticity organization in the outer layer of turbulent channels with disturbed walls. *J. Fluid Mech.*, **591**:145–154, 2007.
[2] J. Jiménez. Coherent structures in wall-bounded turbulence. *J. Fluid Mech.*, **842**:P1, 2018.
[3] A. G. Kidanemariam and M. Uhlmann. Interface-resolved direct numerical simulation of the erosion of a sediment bed sheared by laminar channel flow. *Int. J. Multiphase Flow*, **67**:174–188, 2014.
[4] I. Marusic, R. Mathis, and N. Hutchins. Predictive model for wall-bounded turbulent flow. *Science*, **329**(5988):193–196, 2010.
[5] I. Nezu and H. Nakagawa. *Turbulence in open channels*. IAHR/AIRH Monograph. Balkema, Rotterdam, The Netherlands, 1993.
[6] A. A. Townsend. *The structure of turbulent shear flow*. Cambridge Univ. Press, Cambridge, 2 edition, 1976.
[7] M. Uhlmann. An immersed boundary method with direct forcing for the simulation of particulate flows. *J. Comput. Phys.*, **209**(2):448–476, 2005.

INVESTIGATING THE INTERACTION BETWEEN TURBULENT FLOWS AND SUSPENDED PARTICLES WITH THE AID OF INVARIANT SOLUTIONS

Markus Uhlmann[1], Tiago Pestana[1], Michael Krayer[1] and Genta Kawahara[2]

[1]*Institute for Hydromechanics, Karlsruhe Institute of Technology, 76131 Karlsruhe, Germany.*
E-mail: markus.uhlmann@kit.edu, tiago.pestana@kit.edu, michael.krayer@kit.edu
[2]*Graduate School of Engineering Science, Osaka University, Osaka 560-8531, Japan*
E-mail: kawahara@me.es.osaka-u.ac.jp

Particulate flow systems exhibit a number of puzzling phenomena with important practical consequences. One prominent example is their non-trivial spatial distribution which sometimes manifests itself in the form of clustering and/or preferential concentration with respect to turbulent flow structures [1]. This "de-mixing" of the dispersed phase can significantly affect the operation of diverse processes, such as chemical reactions, heat transfer, growth of droplets in clouds, etc. Modern laboratory experiments and high-fidelity numerical simulations have enabled researchers to gather an enormous wealth of data, with the aid of which a number of aspects pertaining to particle-turbulence interaction have already been elucidated. However, many other questions still elude our understanding, e.g. how to disentangle the roles of density and particle size in determining the particle dynamics.

In order to simplify the problem, we propose to study particles suspended in simple invariant solutions (equilibria, periodic orbits) to the Navier-Stokes equations. Since these flows are believed to be relevant to turbulence [2], they allow us to design tractable numerical laboratories for the investigation of particle dynamics. In a first step we have demonstrated the feasibility of this approach by using Nagata's equilibrium solution in Couette flow for this purpose [3]. It could be shown that the well-known focusing of heavy particles into low-speed streaks (and subsequent apparent velocity lag) can be captured in this manner. Subsequently we have started to explore a number of solutions in different flow configurations: open channel flow, rectangular duct flow, homogeneous flow under different types of forcing. In addition to using equilibrium solutions, we have also employed periodic orbits, both in wall-bounded and unbounded flows.

At the workshop we are going to report on our ongoing research in this direction. We will discuss the stability of the respective invariant solutions with respect to the addition of finite-size particles, as well as our attempts to extract new physics from these systems.

Figure 1. Trajectory of a spherical particle (diameter $D/h = 0.16$, density ratio $\rho_p/\rho_f = 10$) suspended in the "gentle" Couette periodic orbit of [4] at $Re = 250$ and zero gravity. The temporal interval corresponds to approximately 500 bulk time units. The view is into the streamwise direction (left) and into the span (right); the grey-colored boxes indicate the domain size, while the trajectory is unwrapped in the periodic directions.

References

[1] S. Balachandar and J.K. Eaton. Turbulent dispersed multiphase flow. *Ann. Rev. Fluid Mech.*, 42:111–133, 2010.

[2] G. Kawahara, M. Uhlmann, and L. van Veen. The significance of simple invariant solutions in turbulent flows. *Ann. Rev. Fluid Mech.*, 44:203–225, 2012.

[3] T. Pestana, M. Uhlmann, and G. Kawahara. Can preferential concentration of finite-size particles in plane Couette turbulence be reproduced with the aid of equilibrium solutions? *Phys. Rev. Fluids*, 5:034305, 2020.

[4] G. Kawahara and S. Kida. Periodic motion embedded in plane Couette turbulence: regeneration cycle and burst. *J. Fluid Mech.*, 49:291–300, 2001.

SCALING AND SPATIO-TEMPORAL CONSTRAINTS OF THE MINIMAL SEED IN BOUNDARY-LAYER FLOWS

Emanuel Taschner[1,2], Miguel Beneitez[1,3], Yohann Duguet[4], and Dan S. Henningson[1]
1. FLOW Centre and Swedish e-Science Research Centre (SeRC), KTH Engineering Mechanics, Royal Institute of Technology, SE-100 44 Stockholm, Sweden
2. Delft Center for Systems and Control, Delft University of Technology, 2628CD Delft, The Netherlands
3. DAMTP, Centre for Mathematical Sciences, Wilberforce Road, Cambridge CB3 0WA, UK
4. ISN-CNRS, Campus Universitaire d'Orsay, Université Paris-Saclay, F-91400, Orsay, France

Bypass transition to turbulence is a very sensitive phenomenon, whose accurate prediction can have important repercussions in aeronautical design. Even formulated as an initial value problem, a causal explanation for the seemingly random occurrence of turbulent spots remains yet incomplete. The initial condition energetically closest to the laminar state, while just able to cause transition to turbulence, is called minimal seed [1]. This elegant concept was initially introduced for parallel shear flows, where a given geometry and Reynolds number entirely define the minimal seed. Such a picture is challenged in spatially developing flows [2]. Using nonlinear adjoint optimisation, we show how the resulting minimal seed in spatially developing boundary layer flows depends explicitly on three optimisation parameters: the inlet Reynolds number at the start of the computational domain, the horizon time and the dimensions of the computational domain. Our results suggest a new scaling for the energy of the minimal seed with the Reynolds number, other parameters being held constant. We analyse the physical structure of the minimal seed for several Reynolds numbers by classifying patterns of high and low streamwise velocity perturbations. Both Orr and lift-up mechanisms can be singled out during the temporal evolution of the minimal seeds. We then show that shorter optimisation times result in suboptimal transition.

Financial support by the Swedish Research Council (VR) Grant No. 2016-03541 and computing time provided by the Swedish National Infrastructure for Computing (SNIC) are gratefully acknowledged

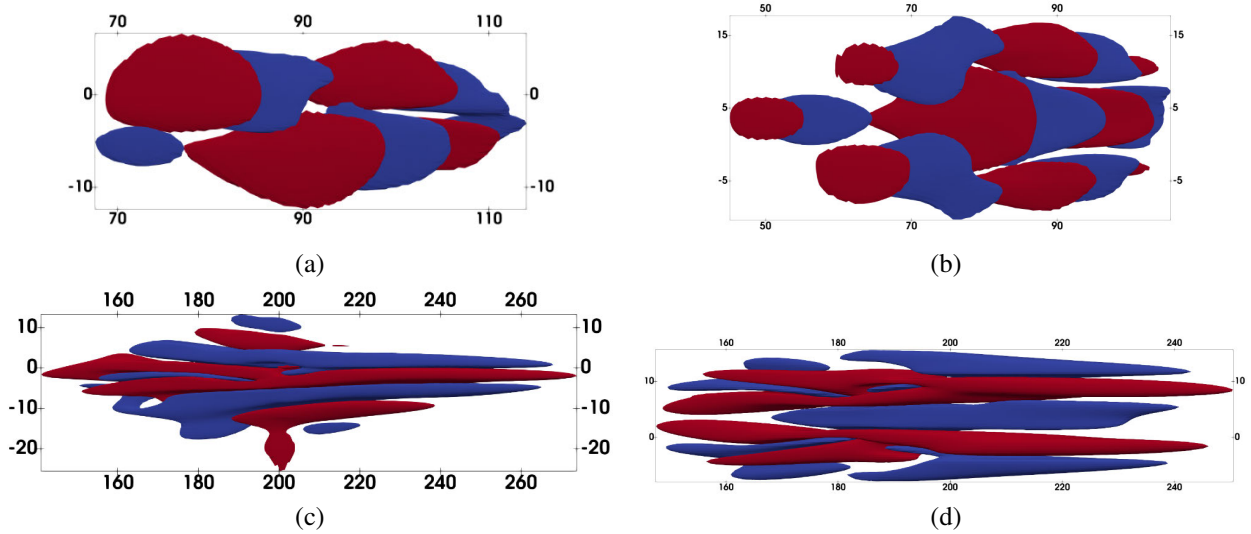

Figure 1. Streamwise perturbation velocity (blue for negative; red for positive) for (a,b) optimal disturbances above the minimal seed in the set-up described in [2]. (a) $E_0 = 1.7 \times 10^{-2}$, $Re_{\delta^*} = 275$ (b) $E_0 = 3.0 \times 10^{-2}$, $Re_{\delta^*} = 395.98$. (c,d) Evolution of perturbations (a,b) at $t = 200$

References

[1] Pringle C. C., Willis A. P., and Kerswell R. R., Minimal seeds for shear flow turbulence: Using nonlinear transient growth to touch the edge of chaos, *J. Fluid Mech.*, vol. **702**, 415-–443, 7 (2012)

[2] Vavaliaris C., Beneitez M., and Henningson D. S., Optimal perturbations and transition energy thresholds in boundary layer shear flows, *Phys. Rev. Fluids*, **5**, 062401(R) (2020).

CAUSAL INFERENCE, CAUSAL DISCOVERY, AND MACHINE LEARNING

Jakob Runge
Causal Inference group, Institute of Data Science, German Aerospace Center, Jena, Germany
E-mail: Jakob.Runge@dlr.de

In the past decades machine learning has had a rapidly growing impact on many fields of natural-, life- and social sciences as well as engineering. Machine learning excels at classification and regression tasks from complex heterogeneous datasets and can answer questions like "What statistical associations or correlations can we see in the data?", "What objects are in this picture?", or "What is the most likely next data point?". But many questions in science, engineering, and politics are about "What are the causal relations underlying the data?" or "What if a certain variable changes or is changed?" or "What would have happened if some variable had another value?". Data-driven machine learning alone fails to answer such questions. Causal inference provides the theory and methods to learn and utilize qualitative knowledge about causal relations. Together with machine learning it enables causal reasoning given complex data. Furthermore, causal methods can be used to intercompare and validate physical simulation models. In this talk I will present an overview of this exciting and widely applicable framework and illustrate it with some examples from Earth sciences and beyond.